Project Collection

POLITECNICO
MILANO 1863

Energy Conversion A

2022/2023

Gianluca Valenti

Giuseppina Lana 10580348

Giacomo Salani 10653713

Giacomo Mastantuono 10576572

Francesca Agostino 10868686

Francesco Nespoli 10621166

PROJECT 1
ECONOMICS OF POWER PLANTS

1. Introduction:

The scope of the following document is to perform an economic comparison between different power generation technologies. For each plant, the economic analysis highlights the total annual cost as function of the annual equivalent operating hours. Particularly, in the first step, only the annual specific costs are considered and then, in the second step, implemented together along with incentives, externalities and carbon tax costs. In the last section, for a single plant, a sensitivity analysis on the LCOE of the plant varying the price of the natural gas is reported.

2. Data:

Power Plants

Hydroelectric	Hydroelectric pumped storage power plant	
PWR	Nuclear power plant with Pressurized Water Reactor	
NGCC	Natural Gas-fired Combined Cycle	
HDGT	Natural gas-fired Heavy-Duty Gas Turbine in simple cycle	
ADGT	Natural gas-fired Aero-Derivative Gas Turbine in simple cycle	
NGSC	Natural Gas-fired Steam Cycle	
CHP	Combined Heat and Power, natural gas fired Combined Cycle	
PCSC +FGD	Pulverized Coal Steam Cycle + Flue Gas Desulphurization	
USC+ FGD	Pulverized Coal Ultra-Super Critical Steam Cycle+ Flue Gas Desulphurization	
CSP	Concentrated Solar Power Plant (Parabolic trough, diathermic oil, steam cycle)	
Wind	On-shore wind	wind speeds: *8 m/s*
	farm	wind speeds: *16 m/s*

Power Plant technology	Investment Cost (IC)	Carrying Charge Fraction (CCF)	Typical equivalent hours	Operation & Maintenance Costs (O&M)		Nominal electric efficiency $\eta_{e,nom}$
	(€/kWnom)	(1/y)	(h/y)	Fixed (€/kWnom y)	Variable (€/MWhe)	----
Hydroelectric	700	0.0905	3000	11	1	0.71
PWR	4000	0.0989	7600	53	1.5	0.35
NGCC	600	0.1053	8000	12.3	1.2	0.61
HDGT	250	0.1009	8000	6	9	0.35
ADGT	300	0.1009	8000	8	9	0.40
NGSC	800	0.1076	7500	13	2	0.41
CHP	700	0.1175	5500	16	1.5	0.43
PCSC+FGD	1300	0.1124	7500	17.5	2.5	0.39
USC+FGD	1450	0.1124	7500	17.5	3	0.44
CSP	2700	0.0977	2100	11	3	0.25
Wind (8 m/s)	6600	0.1053	2000	8	0.2	0.42
Wind (16 m/s)	820	0.1053	2000	8	0.2	0.42

Power Plants Characteristics

Fuel Characteristics

Compositions and heating values

Weight fraction				LHV	(MJ/kg)	MM	(kg/kmol)
Natural Gas		Coal					
Specie	Mi%	Specie	Mi%	CH_4	50	CH_4	16.04
CH_4	94%	C	62%	C_2H_6	47.5	C_2H_6	30.07
C_2H_6	4%	H_2	3%	Coal	23.9	C	12.011
N_2	2%	S	1%			S	32.066
		O_2	6%			O_2	32
		N_2	2%			N_2	28.01
		Ash	16%			H_2	2.016
		Humidity	10%			CO_2	44.011
						SO_2	64.066
						NO_2	46

Prices

Fuel	Price	
Natural Gas	0.3	€/m3(standard cond.)
Thermal-use Natural Gas	0.4	€/m3(standard cond.)
Coal (raw material)	65	$/ton
Coal (naval transport)	25	$/ton
Nuclear fuel	1	€/GJth
Electricity for pumped storage	30	€/MWhe

Dollar/Euro exchange rate: 1.00 $/€
Standard conditions: 1 atm and 15°C. Normal conditions: 1 atm e 0°C

Incentives And Externalities

Cost of externalities

Emissions	Cost	
NO_x	3	€/kg
SO_x	3,5	€/kg
Particulate Matter (PM)	15	€/kg
CO_2	30	€/t
Nuclear fuel	0,003	€/kWhe

Specific emissions and flue gas treating systems

Power Plant	NO_x	SO_x	Particulate Matter	CO_2
Hydroelectric	0	0	0	0
PWR	0	0	0	0
NGCC	20 mg/Nm^3 (15%O_2)	0	0	unknown
HDGT	20 mg/Nm^3 (15%O_2)	0	0	unknown
ADGT	20 mg/Nm^3 (15%O_2)	0	0	unknown
NGSC	50 mg/Nm^3 (3%O_2)	0	0	unknown
CHP	20 mg/Nm^3 (15%O_2)	0	0	unknown
PCSC+FGD	80 mg/Nm^3 (6% O_2)	unknown (capture 95%)	10 mg/Nm^3 (6% O_2)	unknown
USC+FGD	80 mg/Nm^3 (6% O_2)	unknown (capture 95%)	10 mg/Nm^3 (6% O_2)	unknown

Profits from incentives

The incentive figures are allocated solely to renewable energy sources power plants; for sake of generalization, an average amount of 70 €/MWh is considered for the first 15 years of operation. Assume an inflation rate of 2% and a discount rate of 9% to distribute over the lifetime.

3. Total Specific Annual Cost Analysis

The annual cost comparison analysis between the technologies listed above is performed in two main phases:

1) Evaluation of the specific annual costs
2) Implementation of the specific annual costs considering incentives, externalities and carbon tax.

Each step of the analysis is reported below in the following paragraphs.

To be noted that we will compare the costs in two ways:

- $\left[{}^{€}/_{kW_{nom,ele}y}\right]$, which is the best comparison when also considering availabilities (h/y) that different technologies can offer,
- $\left[{}^{€}/_{kW_{h,ele}}\right]$, which is the best comparison when availabilities are not considered.

A dimensional analysis shows that these two different comparisons are linked through the annual equivalent operating hours:

$$\left[\frac{€}{kW_{nom,ele}y}\right] = \left[\frac{h}{y}\right] \cdot \left[\frac{€}{kW_{h,ele}}\right]$$

3.1 Specific annual cost

In the first step, we evaluated the specific annual cost for each plant in order to compare them.

The specific annual cost can be calculated as a sum between the independent costs from the energy production of the single plant and the variable costs linked to the plant.

$$C_{TOT} = C_{fix} + C_{var} * h \left[\frac{€}{kW_{h,ele}}\right]$$

3.1.1 Fixed Cost

Fixed costs, that are independent on the amount of energy produced by a plant, are strictly linked to two main contributions:

- The yearly fixed operation and maintenance costs $C_{O\&M,fix}$,
- The yearly allocation of investment costs C_{INV}, which considers the length of construction time of the plant, the expected lifetime and other financial parameters.

$$C_{fix} = C_{inv} + C_{O\&M,fix} \left[\frac{€}{kW_{nom,ele}y}\right]$$

The investment costs can be evaluated as follows:

$$C_{INV} = CCF * (INV_{TOT}) \left[\frac{€}{kW_{nom,ele}y}\right]$$

Where:

- The INV_{TOT} represents the total overnight costs and it is evaluated as the sum of the overnight investment of the plant of the field and insurance.
- The CCF stands for the Carrying Charge Factor, which allocates the fraction of investment to each year. This factor depends on the length of the plant construction period, on its expected lifetime and on financial parameters such as inflation rate, profit rates and interest rates on the invested capital; on the other hand, the overall investment cost does not affect the CCF.

Meanwhile, the fixed operation and maintenance costs are dates known.

The following table reports the C_{fix} computed for each plant:

Power Plants	Investment Cost (IC) (€/kW$_{nom}$)	INV$_{INSURANCE}$ (€/kW$_{nom}$)	INV$_{FIELD}$ (€/kW$_{nom}$)	INV$_{TOT}$ (€/kW$_{nom}$)	CCF (1/y)	C$_{INV}$ (€/kW$_{nom}$y)	O&M$_{fixed}$ (€/kW$_{nom}$y)	Cfix (€/kW$_{nom}$y)
Hydroelectric	700	7	14	721	0.0905	65.2505	11	76.2505
PWR	4000	40	80	4120	0.0989	407.468	53	460.468
NGCC	600	6	12	618	0.1053	65.0754	12.3	77.3754
HDGT	250	2,5	5	257,5	0.1009	25.98175	6	31.98175
ADGT	300	3	6	309	0.1009	31.1781	8	39.1781
NGSC	800	8	16	824	0.1076	88.6624	13	101.6624
CHP	700	7	14	721	0.1175	84.7175	16	100.7175
PCSC+FGD	1300	13	26	1339	0.1124	150.5036	17.5	168.0036
USC+FGD	1450	14,5	29	1493.5	0.1124	167.8694	17.5	185.3694
CSP	2700	27	54	2781	0.0977	271,7037	11	282.7037
Onshore Wind (8 m/s)	6600	66	132	6798	0.1053	715.8294	8	723.8294
Onshore Wind (16m/s)	820	8,2	16,4	844.6	0.1053	88.93638	8	96.93638

To be noted that the field purchase costs (approximately 2% of the IC) and the insurance and the general expenses (approximately 1% of the IC) have to be added to the investment costs of every power plant.

3.1.2 Variable Cost

Variable costs, which are strictly linked to the working time of the plant, can be computed as follows:

$$C_{var} = \left(C_{fuel} + C_{O\&M,var}\right) * h_{eq} \left[\frac{€}{kW_{h,ele}y}\right]$$

Where: $C_{O\&M,var}$ is the variable operational and maintenance costs $\left[\frac{€}{kWh_{el}}\right]$,$C_{fuel}$ stands for the fuel costs $\left[\frac{€}{kWh_{el}}\right]$,$h_{eq}$ is the equivalent operating hours $\left[\frac{h}{y}\right]$.

To be noted that the variable operational and maintenance costs and the equivalent operating hours are given.

The fuel costs can be computed as follows:

$$C_{fuel} = \frac{p_{fuel}}{\overline{\eta_{ele}}} \left[\frac{€}{kWh_{el}}\right]$$

Where:

- The p_{fuel} is the price of the fuel closely linked to the type of fuel used,
- The $\overline{\eta_{ele}}$ is the integral electrical typical efficiency of the plant, which is subject to the aging and partial operation of the plant.

For all plants, the fuel costs evaluation is reported below:

(a) Hydroelectric: The fuel costs for the Hydro plant account the electricity used for pumping storage of water. The fuel price is known in $[€/MWh_{el}]$,which means that to have them in $€/kWh_{el}$, the only conversion factor from MWh to kWh=1000 has to be considered.
The $\overline{\eta_{ele}}$ coincides with the nominal electrical efficiency $\eta_{e,nom}$ because the plant has no efficiency penalties ($\Delta\eta_{el}$).

(b) PWR: The fuel costs for the PWR plant are addressed by the nuclear fuel price. The fuel price is given in $[€/GJ_{th}]$, that means the final cost in $€/kWh_{el}$ can be computed just accounting the conversion factor from GJ to kWh = $3{,}6 * 10^{-3}$.
The $\overline{\eta_{ele}}$ is equal to $\eta_{e,nom}(1 - \Delta\eta_{el})$. The efficiency penalties considered are around 3%.

(c) Natural gas plant: The fuel costs for these four plants are dependent by the natural gas fuel price.
NGCC
HDGT
ADGT
NGSC
The natural gas price is given in $[€/m^3]$, which means to convert it in $[€/kWh_{el}]$,the computations under reported are necessary.

1) Specific volume computation in standard conditions

$$v^* = \frac{v_{standard}}{MM_{naturalgas}} \left[\frac{m^3 * kmol_{natgas}}{kg_{natgas}}\right]$$

With:

$$MM_{natgas} = \left(\frac{y_{CH_4}}{MM_{CH_4}} + \frac{y_{C_2H_6}}{MM_{C_2H_6}} + \frac{y_{N_2}}{MM_{N_2}}\right)^{-1} \left[\frac{kg_{natgas}}{kmol_{natgas}}\right]$$

where y_i is the mass fraction of i-species.

2) Low heating value calculation

$$LHV_{natgas} = \left(y_{CH_4} \cdot LHV_{CH_4} + y_{C_2H_6} \cdot LHV_{C_2H_6} + y_{N_2} \cdot LHV_{N_2}\right) \left[\frac{MJ_{th}}{kg_{natgas}}\right]$$

3) Price of natural gas evaluation

$$p_{natgas,plant} = \frac{p_{natgas} \cdot v^*}{LHV_{natgas}} \cdot 3{,}6 \quad \left[\frac{€}{kWh_{el}}\right]$$

The $\overline{\eta_{ele}}$ is equal to $\eta_{e,nom}(1 - \Delta\eta_{el})$.
The efficiency penalties considered vary for each plant.
For the HDGT and ADGT, which are gas turbine-based power plant, the $\Delta\eta_{el}$ is about 5%.
For the NGSC, which is a steam turbine-based power plant, the $\Delta\eta_{el}$ is about 3%.
For combined cycle as the NGCC, the $\Delta\eta_{el}$ is attributable for two thirds to the gas turbine and for one third to the steam turbine and sits at around 4,3%.

(d) CHP: The fuel cost for a combined heat and power natural gas cycle evaluation is slightly different compared to the one used for other natural gas plants because the CHP produces both electric and thermal power.
The fuel costs can be calculated as a difference between the fuel cost linked to the electricity and that associated to the thermal energy:

$$C_{fuel\ CHP} = \frac{p_{natgas,el}}{\bar{\eta}_{el}} - \frac{p_{nat\ gas,th}}{\eta_{boiler}} \cdot \frac{\eta_{th}}{\bar{\eta}_{el}} \left[\frac{€}{kWh_{el}}\right]$$

Where:

- $p_{natgas,el}$ is the price of the natural gas used for electric power production. It coincides with the one considered for the other natural gas plants.
- $p_{nat\ gas,th}$ is the price of the natural gas due to the thermal power production. The price is given in $[€/m^3]$, which means that the same expression used above can be utilized to convert it in $[€/kWh_{el}]$.
- The $\overline{\eta_{ele}}$ is equal to $\eta_{e,nom}(1 - \Delta\eta_{el})$. The efficiency penalties considered is about 4,3%.
- The annual thermal efficiency and reference thermal efficiency considered are respectively 33% and 90%.

(e) Steam Coal Cycle:
PCSC + FGD
USC

The fuel costs for these two plants are subject to the price of a coal fuel. The coal fuel price is the sum of the price of the raw material at the site where it is mined, plus the price for its naval shipment.
The sum is known in $[\$/ton]$, which means to convert it in $[€/kWh_{el}]$ as follow:

$$p_{coal} = \frac{(p_{mat} + p_{trasp})}{1000} \cdot \frac{1}{LHV_{coal}} \cdot 3{,}6 \left[\frac{€}{kWh_{el}}\right]$$

The $\overline{\eta_{ele}}$ is equal to $\eta_{e,nom}(1 - \Delta\eta_{el})$. The efficiency penalties considered are about 3%.

(f) Renewable sources cycle:
CSP
WIND

The fuel costs are absent for the innovative renewables

The following table summarizes the variable cost results:

Power Plant technology	Price of fuel (€/kWh$_{el}$)	Typical equivalent hours (h/y)	O&M$_{variable}$ (€/MWh$_{el}$)	$\overline{\eta_{ele}}$ ----	Fuel Cost (€/kWh$_{el}$)	Variable Costs (€/kWh$_{el}$)
Hydroelectric	0.03	3000	1	0.71	0.04225	0.04325
PWR	0.0036	7600	1.5	0.3395	0.01060	0.01210
NGCC	0.09174	8000	1.2	0.58357	0.15720	0.15840
HDGT	0.09174	8000	9	0.3325	0.27588	0.28490
ADGT	0.09174	8000	9	0.38	0.24141	0.25041
NGSC	0.09174	7500	2	0.3977	0.23067	0.23267
CHP	0.09174 0.04223	5500	1.5	0.41137	0.18537	0.18687
PCSC+FGD	0.01356	7500	2.5	0.3783	0.03584	0.03834
USC+FGD	0.01356	7500	3	0.4268	0.03176	0.03476
CSP	---	2100	3	0.2425	0	0.003
Wind (8 m/s)	---	2000	0.2	0.4074	0	0.0002
Wind (16 m/s)	---	2000	0.2	0.4074	0	0.0002

3.1.3 Specific annual cost results

At this stage, for each plant the total costs can be computed. The table and the graph below summarizes the results.

Power Plant technology	C_{fix} (€/kW$_{nom}$Y)	C_{var} (€/kWh$_{el}$)	C_{TOT}(€/kWh$_{el}$)
Hydroelectric	76.2505	0.04325	76.2938
PWR	460.468	0.01210	460.48
NGCC	77.3754	0.15840	77.5358
HDGT	31.98175	0.28490	32.2666
ADGT	39.1781	0.25041	39.4285
NGSC	101.6624	0.23267	101.895
CHP	100.7175	0.18687	100.904
PCSC+FGD	168.0036	0.03834	168.042
USC+FGD	185.3964	0.03476	185.404
CSP	282.7037	0.003	282.707
Wind (8 m/s)	723.8294	0.0002	723.83
Wind (16 m/s)	96.93638	0.0002	96.9366

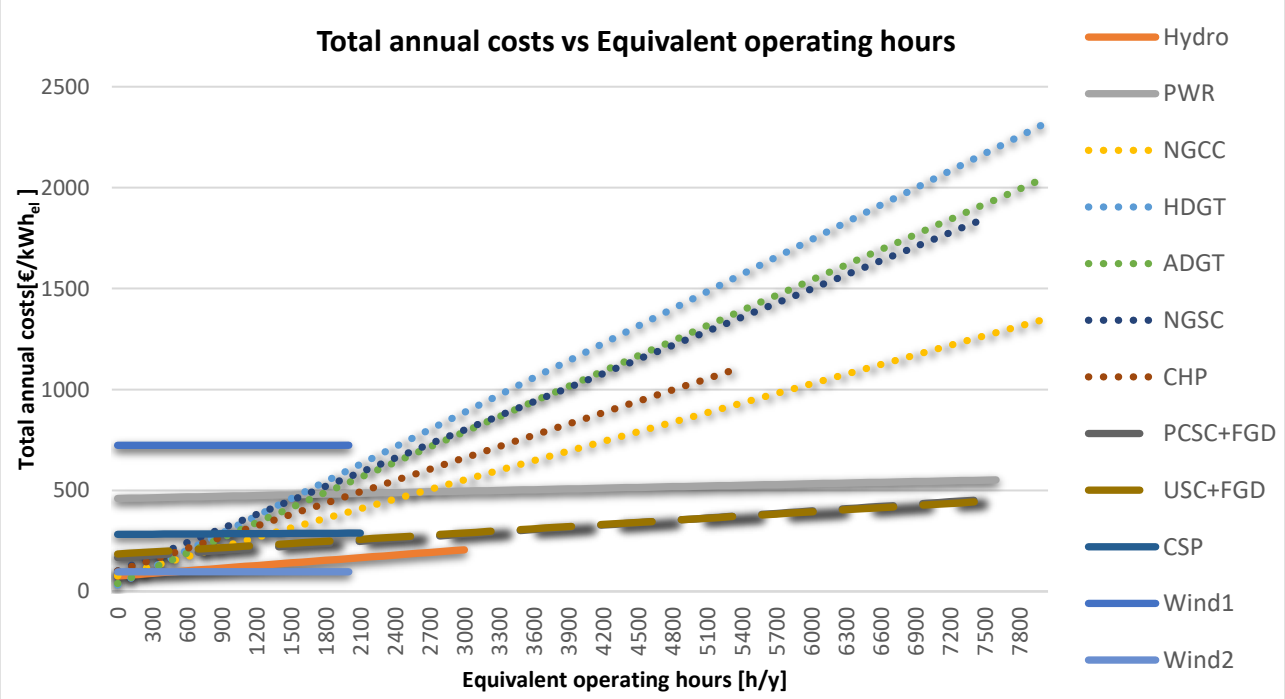

Observing the graph, it is possible underlined that:

- The costs for null operating hours represent the fixed costs of the technologies
- The variable costs of each plant correspond to the slope of each straight line. Therefore, the lower the slope the lower the impact of the variable costs
- The renewable plants are characterized by horizontal lines and therefore they have small variable cost
- The fuel-based plants are characterized by little fixed costs compensated by very high line's slope

3.2 Total specific annual cost analysis with incentives and externalities

In the second step, we implement the specific annual costs considering incentives, externalities and carbon tax.

The specific annual cost can be computed in the same manner explained above.

$$C_{TOT} = C_{fix} + C_{var} * h \left[\frac{€}{kW_{h,ele}}\right]$$

The fixed costs are unchanged compared the previous evaluation.

Meanwhile, the variable costs are subject to additional contributions compared to the computations carried out before. The formula used, in this case, is:

$$C_{var} = \left(C_{fuel} + C_{O\&M,var}\right) * h_{eq} + C_{INC} + C_{CO2} + C_{EXT} \left[\frac{€}{kW_{h,ele}y}\right]$$

Where the additional terms are:

- C_{INC} incentives costs $\left[\frac{€}{kW_{h,ele}y}\right]$
- C_{CO2}carbon tax costs $\left[\frac{€}{kW_{h,ele}y}\right]$
- C_{EXT} externalities costs $\left[\frac{€}{kW_{h,ele}y}\right]$

3.2.1 Incentives

As shown in the graph above, the plants based on renewable sources are characterized by very short periods of use, making them sometimes uncompetitive compared to other technologies.

Some governments choose to reward energy production from innovative renewable technologies in order to make them economically competitive and develop economies of scale.

In order to estimate the costs avoided for producing energy using an innovative renewable power plant (C_{inc}), the following Net Present Value (NPV) method is used:

$$\sum_{n=1}^{15} Revenue_{inc} \frac{(1+i)^n}{(1+a)^n} = \sum_{n=1}^{PP\ lifetime} C_{inc} \frac{(1+i)^n}{(1+a)^n} \left[\frac{€}{kW_{h,ele}y}\right]$$

Where:

- the *Revenue$_{inc}$* is the average amount of incentives about 70 $\left[\frac{€}{MWh}\right]$ considered for the first 15 years of operation
- *i* is the discount rate equal to 9%
- *a* is the inflation rate equal to 2%

The first term of equation is the NPV for the incoming clash flow due to incentives, the second one is for the actual money saving due to incentives. It is important to underline that the effect of incentives should be taken into account with respect to the considered plant lifetime and not only for the incentive time span. Usually, the lifetime of the plant does not match with the incentive time span. For this reason, the

first NPV term is evaluated for the first 15 years, and the second one is calculated over the whole actual lifetime of the power plant.

The following table reports the results obtained:

Renewable power plant	C_{inc} (€/Kwh$_{el}$)
Hydroelectric	0.045
CSP	0.051
Wind	0.055

3.2.2 Externalities and Carbon tax

The externalities costs address the taxes against pollutant emissions. That the term externality indicates the damage caused by the combustion of fossil fuels, in particular the emissions of greenhouse gases to the environment. Specifically in our analysis, emissions of NO_x ,SO_x and CO_2 are addressed along with the computation of carbon tax which goes against harmful greenhouse gases.

As the definition of externalities, these costs refer only to technologies based on fossil fuel (natural gas or coal).

The evaluation of externalities and carbon tax is obtained as follow:

$$C_{ext} = \overline{m_{fuel}} * \overline{y_i} * c_{ext,i} \left[\frac{€}{kW_{h,ele}y}\right]$$

Where:

- $\overline{m_{fuel}} \left[\frac{kg_{fuel}}{kW_{h,ele}}\right]$ is the specific fuel consumption
- $\overline{y_i} \left[\frac{kg_i}{kg_{fuel}}\right]$ is the flue gases composition
- $c_{ext,i}$ $\left[\frac{€}{kg_i}\right]$is the cost of gases composition externalities

The costs of gases composition externalities are known.

The specific fuel consumption is calculated in this way, considering the fuel's mass required to produce the considered base of calculation power output (1 kWh$_{el}$).

$$\overline{m_{fuel}} = \frac{1}{LHV_i * \overline{\eta_{ele}}_{plant} * 3{,}6} \left[\frac{kg}{kWh_{el}}\right]$$

Where: LHV_i depends on the type of fuel considered (natural gas or coal) and the $\overline{\eta_{ele}}_{plant}$ is the integral electrical efficiency of the plant. Both values have already been calculated in the previous steps.

The flue gases composition is determined by the type of fuel used in the plant therefore by its combustion reaction. The evaluations for both natural gases and coal is reported below:

To be noted that the following assumption are made:

1) The reaction occurs under stoichiometry conditions and its complete
2) The air composition given is described as follows: 21% of O_2 and 79% of N_2
3) Ideal gas behaviour

a) Natural gas fuel: Starting from the natural gas reactions of combustion:

$$CH_4 + 2O_2 \rightarrow CO_2 + 2H_2$$
$$C_2H_6 + \frac{7}{2}O_2 \rightarrow 2CO_2 + 3H_2O$$

The only emissions considered are CO_2 and NO_x:

- $y_{CO_2} = n_{CO_2} MM_{CO_2} \left[\frac{kg_{CO_2}}{kg_{fuel}}\right]$
- $y_{NO_x} = v_{DAF,O_2\%}[C_{NO_x}] \left[\frac{mg_{NO_x}}{kg_{fuel}}\right]$

All the stages to evaluate y_i are under reported:

1) inlet molar quantities specific to fuel mass:
$$n_{CH4} = \frac{x_{CH4}}{MM_{CH4}} \left[\frac{kmol}{kg_f}\right]$$
$$n_{C_2H_6} = \frac{x_{C_2H_6}}{MM_{C_2H_6}} \left[\frac{kmol}{kg_f}\right]$$
2) outlet molar quantities specific to the fuel mass are computed:
$$n_{CO_2} = n_{CH_4} + 2n_{C_2H_6}$$
$$n_{O_2} = 2n_{CH_4} + \frac{7}{2}n_{C_2H_6}$$
$$n_{N_2} = n_{N_{2,air}} + n_{N_{2,fuel}}$$
3) Dry ash- free air flue gas molar quantity and its equivalent in $\left[\frac{Nm^3}{kg_f}\right]$
$$n_{DAF} = n_{CO_2} + n_{N_2} \left[\frac{kmol}{kg_f}\right]$$
$$v_{DAF} = n_{DAF} \cdot 22.414 \left[\frac{Nm^3}{kg_f}\right]$$
To be noted that the coefficient 22.414 corresponds to the 1 mole volume in standard condition.
4) Actualization of the specific emission from the stoichiometric condition to the specific conditions given.
$$v_{DAF,O_{2,\%}} = v_{DAF} \cdot \frac{21 - x_{O_2}^{st}}{21 - x_{O_2}^{ref}} \left[\frac{Nm^3}{kg_f}\right]$$
Where: $x_{O_2}^{st} = 0$ because the stoichiometric condition is considered and $x_{O_2}^{ref}$ depends directly on the plan.

b) Coal fuel: Starting from the coal reactions of combustion:

$$C + O_2 \rightarrow CO_2$$
$$H_2 + \frac{1}{2}O_2 \rightarrow H_2O$$
$$S + O_2 \rightarrow SO_2$$

The emissions considered are CO_2, NO_x, SO_2 and PM:

- $y_{CO_2} = n_{CO_2} MM_{CO_2} \left[\frac{kg_{CO_2}}{kg_{fuel}}\right]$

- $y_{NO_x} = v_{DAF,O_2\%}[C_{NO_x}] \left[\frac{mg_{NO_x}}{kg_{fuel}}\right]$
- $y_{SO_2} = n_{SO_2} MM_{SO_2} \left[\frac{kg_{SO_2}}{kg_{fuel}}\right]$
- $y_{PM} = v_{DAF,O_2\%}[C_{PM}] \left[\frac{mg_{PM}}{kg_{fuel}}\right]$

All the stages to evaluate y_i are under reported:

1) inlet molar quantities specific to fuel mass:

$$n_C = \frac{x_C}{MM_C} \left[\frac{kmol}{kg_f}\right]$$
$$n_{H_2} = \frac{x_{H_2}}{MM_{H_2}} \left[\frac{kmol}{kg_f}\right]$$
$$n_{S_2} = \frac{x_{S_2}}{MM_{S_2}} \left[\frac{kmol}{kg_f}\right]$$
$$n_{O_{2,f}} = \frac{x_{O_{2,f}}}{MM_{O_{2,f}}} \left[\frac{kmol}{kg_f}\right]$$
$$n_{N_{2,f}} = \frac{x_{N_{2,f}}}{MM_{N_{2,f}}} \left[\frac{kmol}{kg_f}\right]$$

2) outlet molar quantities specific to the fuel mass are computed:

$$n_{CO_2} = n_C$$
$$n_{O_2} = n_C + \frac{1}{2} n_{H_2} + n_S - n_{O_{2,fuel}}$$
$$n_{SO_2} = n_S$$
$$n_{H_2O} = n_{H_2} + n_{H_2O}^{fuel}$$

3) Dry ash- free air flue gas molar quantity and its equivalent in $\left[\frac{Nm^3}{kg_f}\right]$

$$n_{DAF} = n_{CO_2} + n_{N_2} + n_{SO_2}(1 - \eta_{capture}) \left[\frac{kmol}{kg_f}\right]$$
$$v_{DAF} = n_{DAF} \cdot 22.414 \left[\frac{Nm^3}{kg_f}\right]$$

To be noted that the water is not considered and $\eta_{capture}$ is known.

4) Actualization of the specific emission from the stoichiometric condition to the specific conditions given.

$$v_{DAF,O_{2,\%}} = v_{DAF} \cdot \frac{21 - x_{O_2}^{st}}{21 - x_{O_2}^{ref}} \left[\frac{Nm^3}{kg_f}\right]$$

Where: $x_{O_2}^{st} = 0$ because the stoichiometric condition is considered and $x_{O_2}^{ref}$ depends directly to the plan.

The following tables report the results obtained:

Power Plants	LHV_i(MJ/kg)	$\overline{\eta_{ele}}$	m_{fuel} (kg/kWh$_{el}$)	$x_{O_2}^{ref}$	$v_{DAF,O_{2,\%}}$(Nm^3/kg_f)
NGCC	48.9	0.5836	0.009734153	15%	40.80776203
HDGT	48.9	0.3325	0.017084292	15%	40.80776203
ADGT	48.9	0.3800	0.014948756	15%	40.80776203
NGSC	48.9	0.3977	0.014283448	3%	13.60258734
CHP	48.9	0.4114	0.013808915	15%	40.80776203
PCSC+FGD	23.9	0.3783	0.030722974	6%	1.642689817
USC+FGD	23.9	0.4268	0.027231727	6%	1.642689817

Power Plants	$C_{ext}NO_x$ (€/Kwh$_{el}$)	$C_{ext}SO_2$ (€/Kwh$_{el}$)	$C_{ext}CO_2$ (€/Kwh$_{el}$)	C_{ext}PM (€/Kwh$_{el}$)	C_{ext} (€/Kwh$_{el}$)
NGCC	2,38337E-05	---	0,000787382	---	0,000811216
HDGT	4,18303E-05	---	0,001381925	---	0,001423755
ADGT	3,66015E-05	---	0,001209184	---	0,001245786
NGSC	2,91438E-05	---	0,001155369	---	0,001184512
CHP	3,38107E-05	---	0,001116984	---	0,001150795
PCSC+FGD	1,21124E-05	0,002148395	0,002093911	7,57025E-06	0,004261989
USC+FGD	1,0736E-05	0,001904259	0,001855967	6,70999E-06	0,003777672

3.2.3 Total specific annual cost analysis with incentives and externalities results

At this stage, for each plant the total costs can be computed considering all the variable costs. The table and the graph below summarize the results.

Power Plant technology	C_{fix} (€/kW$_{nom}$Y)	C_{var} (€/kWh$_{el}$)	C_{ext} (€/Kwh$_{el}$)	C_{inc} (€/Kwh$_{el}$)	C_{TOT}(€/kWh$_{el}$)
Hydroelectric	76.2505	0.04325	---	0.045	76.3387
PWR	460.468	0.01210	0.003	---	460.4831
NGCC	77.3754	0.15840	0.000811216	---	77.5346
HDGT	31.98175	0.28490	0.001423755	---	32.2681
ADGT	39.1781	0.25041	0.001245786	---	39.4298
NGSC	101.6624	0.23267	0.001184512	---	101.8963
CHP	100.7175	0.18687	0.001150795	---	100.9055
PCSC+FGD	168.0036	0.03834	0.004261989	---	168.0462
USC+FGD	185.3964	0.03476	0.003777672	---	185.4079
CSP	282.7037	0.003	---	0.051	282.7578
Wind (8 m/s)	723.8294	0.0002	---	0.055	723.8841
Wind (16 m/s)	96.93638	0.0002	---	0.055	96.9911

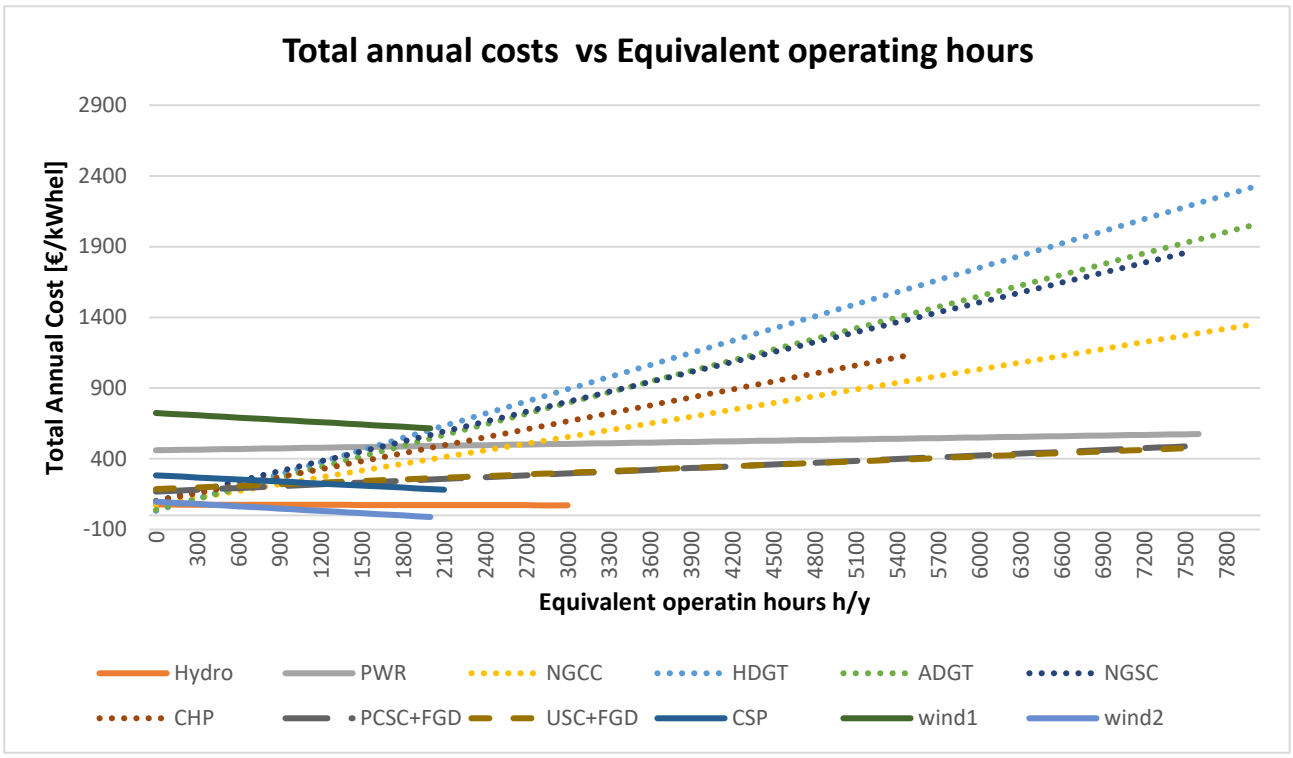

Observing the graph, it is possible underlined that:

- The renewable plants are characterized by negative slopes lines, due to the incentives.
  The Wind 2 plant goes even reaches the brake even Point
- The fuel-based plants are characterized by very high line's slope due to the fuel cost and the taxes for the emissions.

4. Sensitivity analysis

A sensitivity analysis is the study of how the uncertainty in the output of a mathematical model or system (numerical or otherwise) can be divided and allocated to different sources of uncertainty in its inputs.

For the NGCC plant, a sensitive analysis about the Levelized Cost of Energy (LCOE) varying the price of the natural gas in the range of 01/01/2020 – 01/09/2022 is performed.

The following graph summarizes the result obtained:

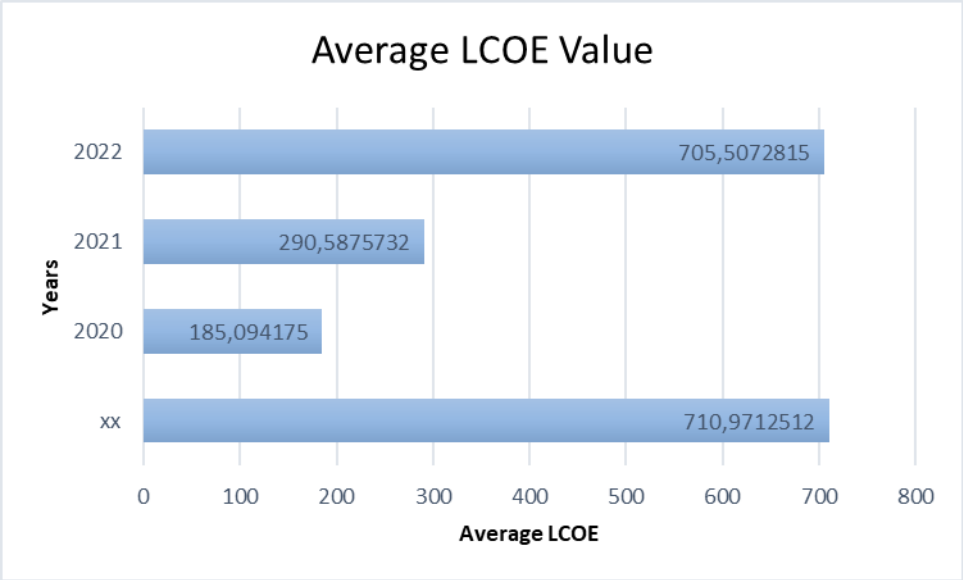

Where the average of the LCOE is reported as a function of years considered. To be noted that xx stands for the case studied above.

The price of the natural gas considered are under reported:

Years	**Price Natural Gas (€/kWh$_e$)**
xx	0.0917
2020	0.0145
2021	0.0305
2022	0.0917

It can be easily noticed that the variation of the fuel price has an important impact on the plant LCOE value. In fact, the LCOE mean value referred to 2022 is quite similar to the one calculated above, as the price of the natural gas is about the same. On the other hand, considering the 2021 or 2020 year, the natural gas price is little less and consequently the LCOE is proportionally below to the xx case.

PROJECT 2
ANALYSIS OF A ONE-PRESSURE LEVEL HEAT RECOVERY STEAM CYCLE

1.Introduction

The aim of the document is to perform a preliminary design of a heat recovery steam cycle with one evaporation level that exploits the energy available in the gas turbine exhaust gases in order to produce additional electric energy. The cycle sketch is reported below.

The analysis is based on three steps:

- Evaluation of the gas turbine outlet temperature modification due to the heat recovery steam generator
- Optimization of the evaporation pressure to maximize the net electrical power
- Second law analysis performance

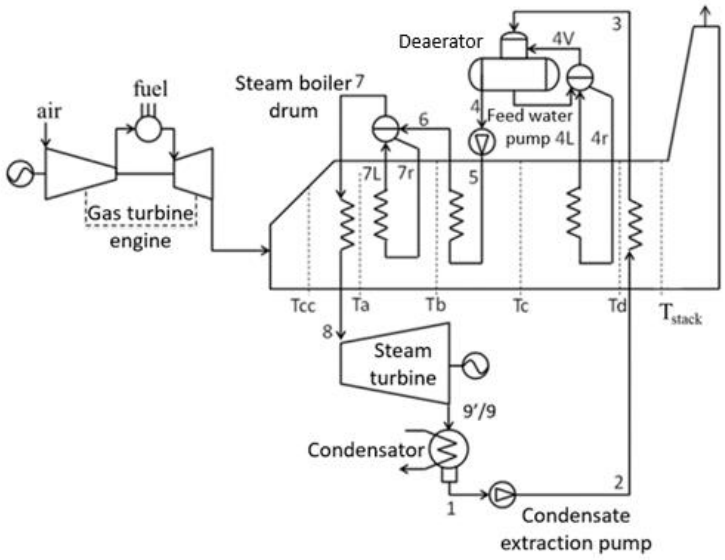

2. Data

Simple cycle gas turbine characteristic

Exhaust gases mass flow rate	659.8 kg/s
Exhaust gases temperature	547.5 °C
Electric power at the electric generation	241.9 MW
Electric efficiency at the electric generator (LHV)	38%

Simple cycle gas turbine assumptions

Molar mass for the exhaust gases	28.4 kg/kmol	
Fourth order polynomial coefficients	$c_p^0 = a_0 + a_1 T^1 + a_2 T^2 + a_3 T^3 + a_4 T^4$	a_0 = 1081.68 a_1 = -0.376266 a_2 = 0.0010736 a_3 = -7.2817576e-7 a_4 = 1.58086e-10

Steam cycle assumptions

Ambient temperature	15 °C	$\eta_{s,ST}$	NOTE
Ambient pressure	101325 Pa	η_{aux}	0.96
Maximum steam turbine	538 °C	$\eta_{s,PMP}$	0.80
Condensing pressure	0.05 bar	$\eta_{el,ST}$	0.985
Deaerator pressure	2.0 bar	$\eta_{mech,ST}$	0.995
Maximum steam pressure	200 bar	$\eta_{th,steamgen}$	0.99
ΔT_{pp}	10 °C	$\eta_{e,m,PMP}$	0.93
ΔT_{ap}	25 °C	$\eta_{el,GT}$	0.99
ΔT_{sc}	10 °C	$\eta_{mech,GT}$	0.995
ΔP_{HRSG}	3000 Pa	$\eta_{s,GT}$	0.925
$\Delta P/P_{eco}$	10%		

NOTE: The steam turbine isentropic efficiency, $\eta s_{,ST}$, is corrected as a function of the outlet steam fraction. The efficiency is constant and equal to 0.93 until the steam fraction equals 0.98. The subsequent expansion process is characterised by a nominal isentropic efficiency (0.93) reduced by a percentage point per each percentage point of outlet liquid fraction less than 2%, throughout the following function: $\eta_{s,ST} = min\,[0.93; 0.93 - (0.98 - \chi_9)]$

3. Evaluation of gas turbine outlet temperature

The simple gas cycle outlet temperature and pressure are influenced by the installation of the heat recovery steam generator (HRSG), as the under reported sketch shows.

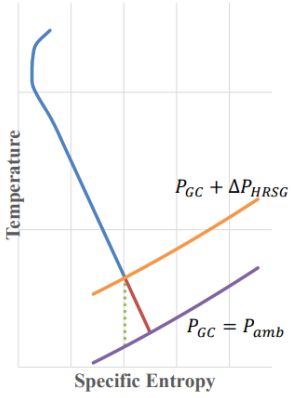

The HRSG is characterized by pressures drops, meaning that the outlet pressure of the gas cycle won't be the ambient pressure as for the simple cycle but will be higher in order to compensate these losses. In the T-S diagram, the purple line stands for the outlet pressure of the gas turbine, while the orange one represents the outlet pressure of the gas turbine considering also the HRSG.

It is important underline that the pressure drop set by the HRSG gives a decrease in the useful enthalpy drop from the gas turbine and therefore the temperature at the turbine outlet is higher.

The new TOT due to the presence of the HRSG is evaluated by an isentropic approach as follows:

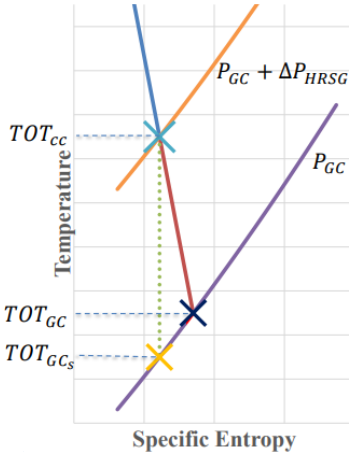

$$\begin{cases} s\left(TOT_{GC,s}, P_{GC}\right) = s\left(TOT_{GC,s}, P_{GC} + \Delta P_{HRSG}\right) \\ \frac{h(TOT_{CC}) - h(TOT_{GC})}{h(TOT_{CC}) - h(TOT_{GCs})} = \eta_{s,GT} \end{cases}$$

To be noted that the approach prosed can be used only where the adiabatic conditions are met. Therefore, it is applied for the last stages of the turbine, which are not cooled.

The system in two equations allows to calculate the two unknowns $TOT_{GC,s}$ and TOT_{CC}.

All the steps are under reported:

- $\eta_{s,GT}$, the TOT_{GC} and the ΔP_{HRSG} are given
- The thermodynamics properties of the exhaust gases are assessed by a VBA based on the polynomial formula given for the specific heat.
  a) Specific heat at the ambient temperature computation:

$$c_p^0(T_0) = a_0 + a_1 T^1 + a_2 T^2 + a_3 T^3 + a_4 T^4$$

  b) Enthalpy and Entropy calculation:

$$h(T_1) = h_0 + a_0(T_1 - T_0) + \frac{a_1}{2}(T_1^2 - T_0^2) + \frac{a_2}{3}(T_1^3 - T_0^3) + \frac{a_3}{4}(T_1^4 - T_0^4) + \frac{a_4}{5}(T_1^5 - T_0^5)$$

$$s(T_1) = s_0 + a_0 \ln\left(\frac{T_1}{T_0}\right) + a_1(T_1 - T_2) + \frac{a_2}{2}(T_1^2 - T_0^2) + \frac{a_3}{3}(T_1^3 - T_0^3) + \frac{a_4}{4}(T_1^4 - T_0^4) + R^* \ln\left(\frac{p}{p_0}\right)$$

The results obtained by a goal-seek function are under reported:

- $TOT_{GC,s}$ = 547,3°C
- TOT_{CC}= 550 °C

4. Optimization of the evaporation pressure to maximize the net electric power output

The thermodynamic proprieties of all the points across the combined gas cycle must be found before moving towards the optimization of such values. The points within the single-phase region must be defined by at least two proprieties for its characteristics to be fully known, whereas those falling in the two-phase region only need one propriety to be fully defined. The given VBA module was widely used to compute the proprieties of water across the whole HRSG.

1. **CONDENSER**
   Always used as the starting point during the analysis of Ranking and combined cycles, its pressure and temperature are both absolute minimums. The pressure was already known, sitting at 0.05 bar, which allowed for the computation of the condensing pressure using Antoine's relation.

$$P_1 = P_{cond}$$

2. **LOW PRESSURE PUMP**
   Being given the Deaerator pressure p3 and the pressure losses across the economizer, which sists in between the said device and the extraction pump, the pressures were simply found as follows:

$$knowing\ \Delta p_{ECO} = 10\%$$
$$deaerator\ pressure\ p_3 = 2\ bar$$
$$p_2 = p_3 * (1 + \Delta p_{ECO}) = 2.2\ bar$$

Using the VABA script, the enthalpies at points 1 and 2s were found, which, by using the given isentropic efficiency of the pump allowed for the computation of h2 as:

$$h_2 = \frac{h_{2s} - h1}{\eta_{s,PMP}} + h1$$

Having know h2 and p2, all the other proprieties are then found using the VABA script.

3. ECONOMIZER

The economizer pressure p_3 has already been defined above while its temperature can be computed by subtracting the ∆T of sub cooling from the temperature T4. T4 itself was calculated using Antoine's relation at p3=p_{dear}=2 bar

$$P_3 = P_{dear}$$

$$T_3 = T_4 - \Delta T_{SC} \; where \; \Delta T_{SC} = 10°$$

4. DEAERATOR

The pressure of this specific point has been widely discussed before.

5. HIGH PRESSURE PUMP

The thought process that went into the calculation for this specific point follows the same reasoning as per point 2, like stated below:

$$p_5 = p_{eva} * (1 + \Delta p_{ECO}) \; and \; thus \; s_{5s} = s_4 \rightarrow h_{5s} \rightarrow h_5 \; being \; \eta_{s,PMP} \; known$$

6. STEAM GENERATOR'S OWN ECONOMIZER

The pressure is given, so that p6=peva and thus T6 can be computed using Antoine's relation and then subtracting the deltaT of sub cooling as stated below

$$T_6 = T^{sat}(p_6) - \Delta T_{SC}$$

7. EVAPORATOR

There is no variation in pressure throughout the evaporator so p_7=p_6 and T_7 was already computed before as

$$T_7 = T^{sat}(p_6)$$

8. SUPERHEATER

The temperature at this point can be computed thanks to the previously found TOT_{cc}-Turbine Outlet Temperature of the exhaust gasses and the ∆T of approach point, which are both known values:

$$T_8 = TOT_{CC} - \Delta T_{ap} = 553 - 25 = 528°C$$

9. EXPANDER OUTLET

Since the project guidelines explicitly state that the steam turbine efficiency changes with respect of the vapor fraction as

$$\eta_{s,ST} = \min\left[0.93; 0.93 - (0.98 - x_9)\right]$$

the expansion must be divided into two different sections:

a) Expansion at constant efficiency between 8-9'

b) Expansion between 9'-9 characterized by variable efficiency, function of the outlet vapor quality as better described above.

a) The vapor quality is fixed at the given value of $x'_9 = 0.98$, which allows for the precise computation of entropy and enthalpy using the known isentropic efficiency.
We start by saying that s9's=s8 , then guessing a p9' value between pcond and p8 which will have to be adjusted later on. Having now both s9's and p9', we can compute the enthalpy using the VABA script, set a goals seek that verify that the resulting efficiency matches the actual given one by the guideline.

$$s'_{9s} = s_8,\ P_9^{\prime(1)} = (1st\ guess, btw\ p\_cond\ \ and\ p\_8) \rightarrow h_{9s}^{\prime(1)} = h\left(P_9^{\prime(1)}, s'_{9s}\right) \rightarrow$$

$$thus\ \eta_{s,TRB} = \frac{h_8 - h_9^{\prime(1)}\left(P_9^{\prime(1)}, x'_9\right)}{h_8 - h_{9s}^{\prime(1)}\left(P_9^{\prime(1)}, s'_{9s}\right)} = 0.93$$

b) The pressure along this section is known, sitting at $p_9=p_{9s}=P_{cond}$. However, the same cannot be stated for the other proprieties, which must be found through the use of an iterative procedure:

i. The x_9 is first guessed, which then leads to x_{9s}

ii. $x_{9s} = x(P_9, s_{9s} = s'_9)$

iii. The isentropic efficiency is obtained as follows:

$$\eta'_{s,TRB} = \eta'_{s,TRB}(x_9) = \frac{h\prime_9 - h_9^{(1)}\left(P_9, x_9^{(1)}\right)}{h\prime_9 - h_{9S}^{(1)}\left(P_9, x_{9S}^{(1)}\right)}$$

It must be said that over the first iteration, all the relating calculations were computed using the maximum evaporation pressure (P_{eva}) of 200 bar.
The last missing key parameter to fully define the system is the mass flow rate of water circulating through the heat recovery steam generator, which was calculated computing an energy balance across the evaporator, as shown below:

$$Energy\ balance: \eta_{th,steam\ gen}\dot{m}_{exh}\int_{T_b}^{TOT_{cc}} c_{p,exh}(T)dT = \dot{m}_w \Delta h_{8-6}$$

The expression above can easily be solved since $\Delta T_{ap}\ and\ \Delta T_{pp}$ were given, so Tb was computed as:

$$T_b = T_6 + \Delta T_{SC} + \Delta T_{PP}$$

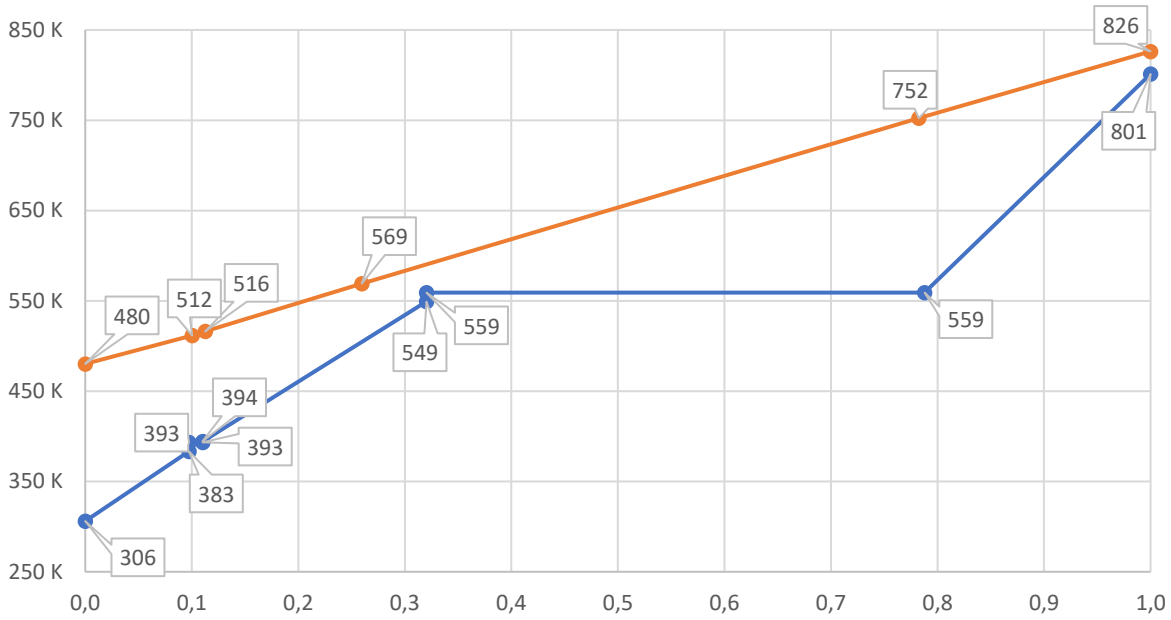

The actual power output of the steam cycle can now be defined as follows:

$$\dot{W_{el,SC}} = \eta_{aux}\, \dot{m_w}\, [\, (\Delta h_{8-9}) * \eta_{el,ST} * \eta_{mech,ST} - \frac{\Delta h_{2-1} \Delta h_{5-4}}{\eta_{em_{pmp}}}\,]$$

Which is basically the net power produced by the steam turbine minus the power absorbed by the operating pumps. Using the above equation, the optimal evaporation temperature can now be found just by maximizing the electric power output through an iterative method.

The optimal evaporation pressure is thus found to be equal to

$$p_{eva,opt} = 70\ bar$$

Listed below is a table containing all the thermodynamical points of the Heat Recovery Steam Generator:

Points	T [K]	P [bar]	h	s	X_v
1	306,0254895	0,05	137,76512	0,476254	0
2is	306,0254895	2,2	137,96905	0,476254	
2	306,0775699	2,2	138,02003	0,47665	
3	383,3615459	2	462,29947	1,421018	
4	393,3615459	2	504,68385	1,530209	0
5is	394,0050833	77,11594654	512,69113	1,530209	
5	394,4804654	77,11594654	514,69295	1,53535	
6	549,0818586	70,10540595	1215,0659	3,027327	
7	559,0818586	70,10540595	2772,4319	5,813688	1
8	801,2286469	70,10540595	3478,9054	6,885013	1
9's	390,5931634	1,830999333	2596,2239	6,885013	0,9520327
9'	390,5930467	1,830999333	2658,0116	7,043202	0,98
9s	306,0254714	0,05	2147,4137	7,043202	0,8294051
9	306,0254239	0,05	2240,4446	7,3472	0,8678

As well as the net power output, turbine efficiency and mass flow rate of steam obtained after the iterative evaluation:

Wel,net [MW]	Kg/s	ηI
93.65	83.98	0.33

The pressure found is mainly dependent, as clearly showed in the equation above, by 2 main parameters: the mass flow rate of water and the enthalpy drop across the steam turbine.
Having sad so, these values are at the same time function of other variables and their relations will be briefly discussed in the next section.

The mass flow rate is indeed strictly related to the evaporation pressure: the higher this goes, the lower the enthalpy of evaporation is going to be, while the superheater and economizer undergo an increase of heat introduction. This process causes a reduction in ΔT between the exhaust gasses entering the HRSG and the water, effectively determining a reduction in mass flow rate of steam created.
On a side note, the increase in evaporation pressure while the ambient pressure stays the same guarantees a higher enthalpy drop across the turbine since the expansion ratio increases, which drives up the net power output.
The relation between evaporation pressure, enthalpy drop, and net electric power output described in the previous page can be better appreciated in the following graph.

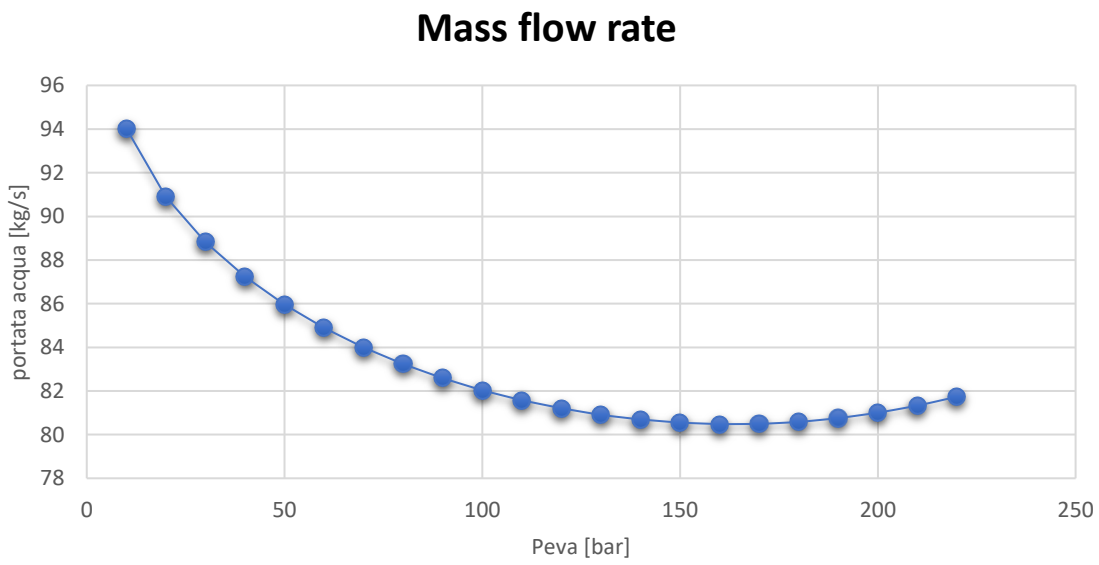

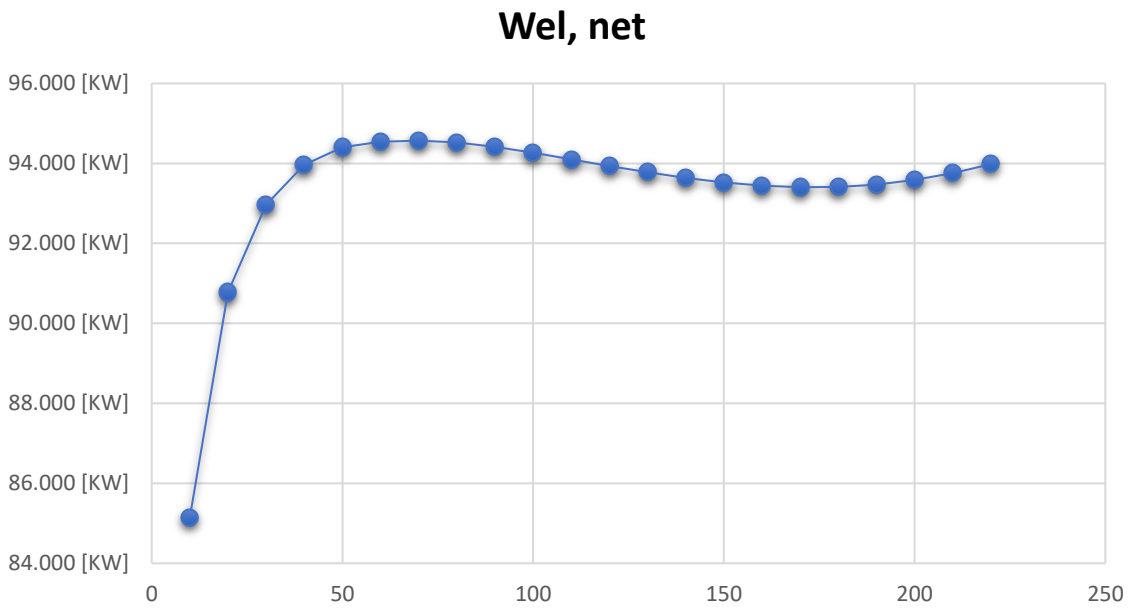

It is clear how relevant the delta in enthalpy is just by looking at the power output: during the first phase the weight of this change is much greater than the one that affects the mass, driving therefore the power generation up until the optimal point, which indeed corresponds to the optimal evaporation pressure, where the power production starts decreasing.

The change in pressure affects the first and second law efficiencies as well, since they are both function of the Net Power Output over, respectively, thermal expenditure and maximum useful effect. In the case of the firs law efficiency, it grows exponentially as the p_{eva} increases, since the power output goes up dramatically in the early stages whereas it starts to decrease in the ending phase since the power output diminishes faster than the decrease in thermal power entering the cycle. The following graph shows the pattern of multiple powers, thermal as well as electrical, during the change in p_{eva}.

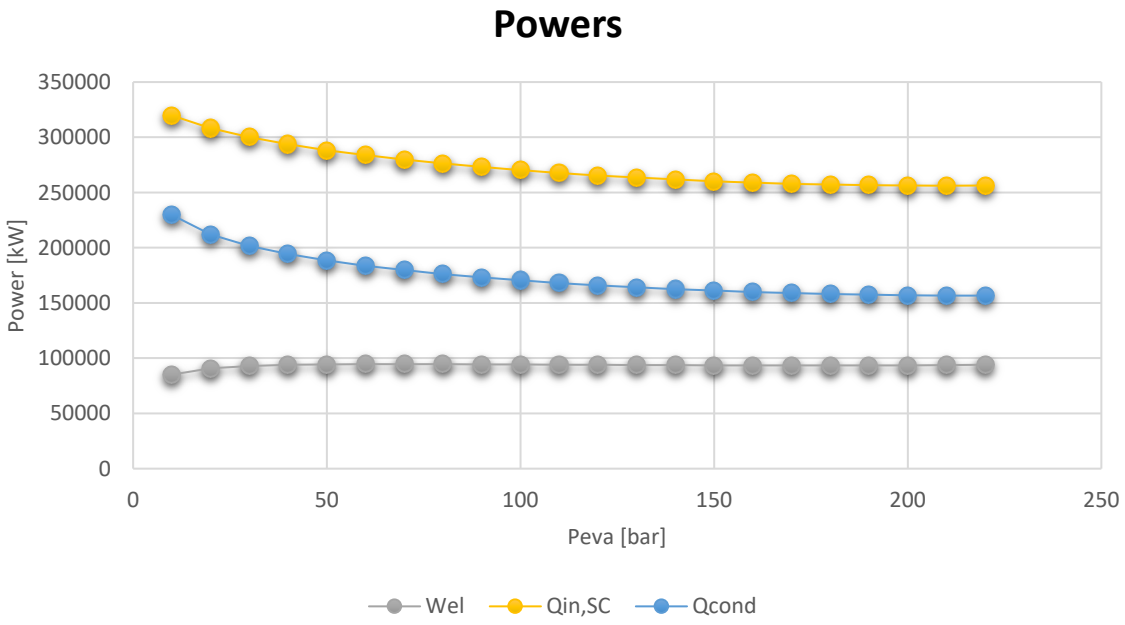

Shown below the 1st and 2nd law efficiencies graph.

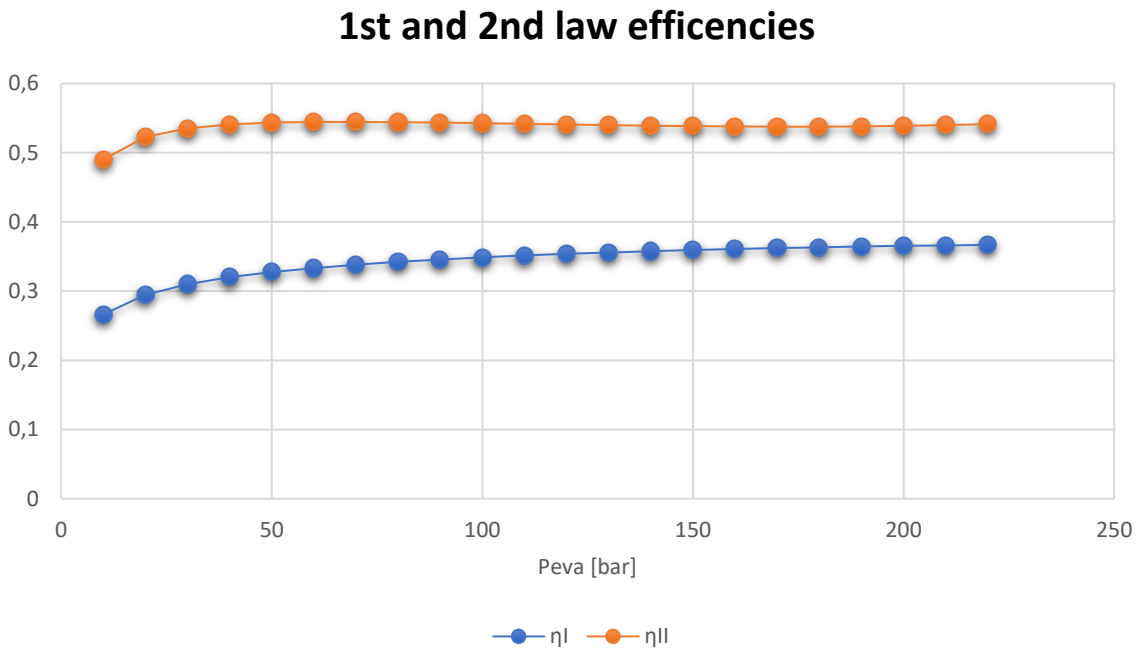

5. Second law analysis performance

In this section the second-law efficiency analysis of the HRSG and the last part of the steam cycle is performed. This analysis quantifies how the energy provided by the exhaust gases of the gas turbine is efficiently used. The general theorem defines for each component j a second-law efficiency loss as it follows:

$$\Delta\eta_{j,II} = T_0 \frac{\Delta\dot{S}_{irr,j}}{\dot{W}_{SC,rev}}$$

$\dot{W}_{SC,rev}$ is the exergy of the exhaust gases that is equal to:

$$\dot{W}_{SC,rev} = \dot{m}_{exh}\{[h(T_{cc}) - h_0] - T_0[s(T_{cc}, P_{cc}) - s_0]\}$$

where $T_0 = 15°C, P_0 = 101325\ Pa,\ h_0 = 0,\ s_0 = 0.$

The aim of this procedure is to estimate the irreversibility of each process in order to improve the system. Finally, it can be assumed that both reaction and mixing irreversibility are negligible with good approximation.

5.1 Fluid dynamic losses

The fluid dynamic losses are generated in the turbomachinery and since the turbomachines of the steam cycle are adiabatic the losses are calculated as entropy generation:

$$\Delta\dot{S}_{irr,j} = \dot{m}_j \Delta\dot{s}_{irr,j} = \dot{m}_j \Delta\dot{s}_j$$

For the steam turbine the losses are:

$$\Delta\dot{S}_{irr,ST} = \dot{m}_w(s_9 - s_8)$$

For the condensate extraction pump the losses are:

$$\Delta\dot{S}_{irr,ST} = \dot{m}_w(s_2 - s_1)$$

For the feed water pump the losses are:

$$\Delta\dot{S}_{irr,ST} = \dot{m}_w(s_5 - s_4)$$

5.2 Electrochemical and auxiliary losses

These losses are generated by the electrochemical conversion and can be estimated as heat exchange losses with the ambient. It can be assumed that the electromechanical components are steady state and at constant entropy, so the losses are estimated as follows:

$$\Delta\dot{S}_{irr,ST} = \frac{\dot{Q}_{diss,e,m,j}}{T_0} + \Delta\dot{S}_{components,j}$$

where $\dot{Q}_{diss,e,m,j} = \left|\dot{W}_{el,j} - \dot{W}_{shaft,j}\right|$.

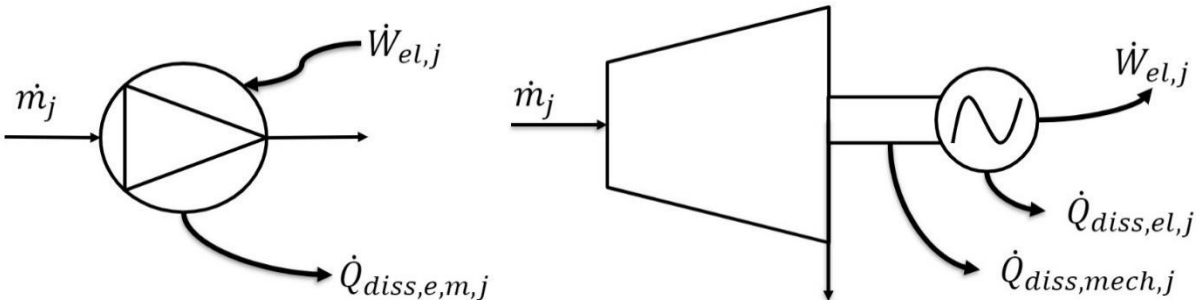

Using the previous expression, the losses for the turbine and the two pumps can be calculated as:

$$\Delta\dot{S}_{irr,el,m,TRB} = \dot{m}_w\left(1 - \eta_{el,ST}\eta_{m,ST}\right)(h_8 - h_9) * \frac{1}{T_0}$$

$$\Delta\dot{S}_{irr,ST} = \dot{m}_w\left(\frac{1}{\eta_{elm,pump}} - 1\right)(h_2 - h_1) * \frac{1}{T_0}$$

$$\Delta\dot{S}_{irr,ST} = \dot{m}_w\left(\frac{1}{\eta_{em,pump}} - 1\right)(h_5 - h_4) * \frac{1}{T_0}$$

The same procedure can be used for auxiliaries:

$$\Delta\dot{S}_{irr,ST} = \dot{m}_w(1 - \eta_{aux})\left(\dot{W}_{el,ST} - \dot{W}_{el,PMPs}\right) * \frac{1}{T_0} =$$

$$= \dot{m}_w[\eta_{el,ST}\eta_{m,ST} * (h_8 - h_9) - ((h_5 - h_4) * \frac{1}{\eta_{em,pump}} - (h_2 - h_1) * \frac{1}{\eta_{em,pump}})]$$

5.3 Heat exchange losses

5.3.1 Stack losses of exhaust gases

The ideal gas law still applies for the calculation of $\Delta\dot{S}_{exh}$, which will be negative because the exhaust gases are cooling down. Instead, the ambient entropy variation will be positive because of the thermal power released by the exhaust gases.

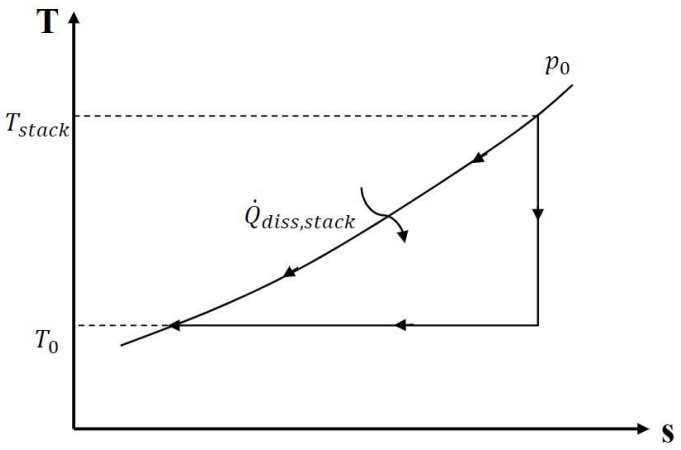

5.3.2 Condenser losses

The condenser process is assumed to be a constant temperature process, so the losses are equal to:

$$\Delta\dot{S}_{irr,cond} = \frac{\dot{Q}_{cond}}{T_0} + \dot{m}_w(s_1 - s_9) = \frac{\dot{m}_w(h_1 - h_9)}{T_0} + \dot{m}_w(s_1 - s_9)$$

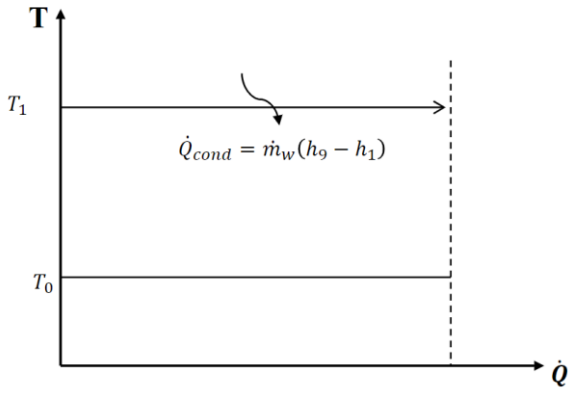

5.3.3 Environment Heat exchange losses

These losses are due to the non-ideal isolation of steam generator because the HRSG isn't adiabatic.

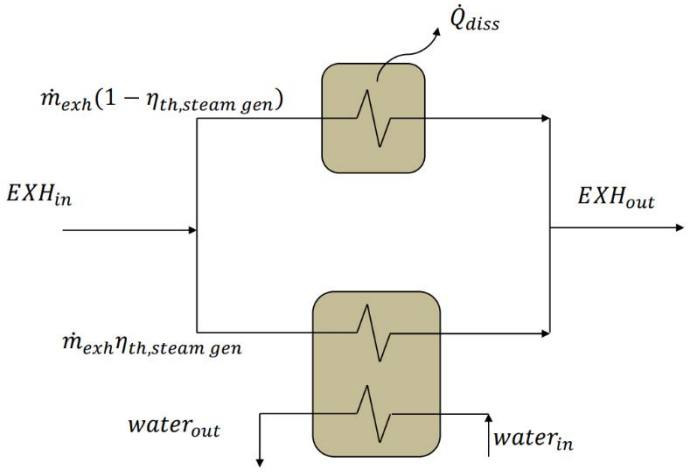

5.3.4 Economizers losses

The losses can be estimated as:

$$\Delta\dot{S}_{irr,ECO1} = \frac{\dot{Q}_{diss,ECO1}}{T_0} + \dot{m}_{exh}\left(1-\eta_{th,SG}\right)[s(T_{stack},P_{cc}) - s(T_d,P_{cc})] =$$

$$= \frac{1}{T_0}[\dot{m}_{exh}\left(1-\eta_{th,SG}\right)(h_d - h_{stack})] + \dot{m}_{exh}\left(1-\eta_{th,SG}\right)[s(T_{stack},P_{cc}) - s(T_d,P_{cc})]$$

The enthalpies h_{stack} and h_d are estimated from the balances:

$$\dot{m}_{exh}\eta_{th,SG}(h_a - h_{stack}) = \dot{m}_w[(h_7 - h_2) - (h_5 - h_4)]$$

$$\dot{m}_{exh}\eta_{th,SG}(h_c - h_d) = \dot{m}_w[(h_5 - h_3) - (h_5 - h_4)]$$

The temperature T_{stack} and T_d can be estimated using the advanced equation of state:

$$\mathrm{h(T_1)} = h_0 + \left[a_0(T_1 - T_0) + \frac{a_1}{2}(T_1^2 - T_0^2) + \frac{a_2}{3}(T_1^3 - T_0^3) + \frac{a_3}{4}(T_1^4 - T_0^4) + \frac{a_4}{5}\left(T_1^5 - T_0^5\right)\right]$$

Also, for the entropies $s(T_{stack},P_{cc})$ and $s(T_d,P_{cc})$ the advanced equation of state can be used:

$$\mathrm{s(T_1)} = s_0 + \left[a_0 \ln\left(\frac{T_1}{T_0}\right) + a_1(T_1 - T_0) + \frac{a_2}{2}(T_1^2 - T_0^2) + \frac{a_3}{3}(T_1^3 - T_0^3) + \frac{a_4}{4}(T_1^4 - T_0^4)\right] - R^* \ln\left(\frac{p}{p_0}\right)$$

5.3.5 Deaerator losses

The losses can be estimated as:

$$\Delta\dot{S}_{irr,DEA} = \frac{\dot{Q}_{diss,DEA}}{T_0} + \dot{m}_{exh}\left(1-\eta_{th,SG}\right)[s(T_d,P_{cc}) - s(T_c,P_{cc})] =$$

$$= \frac{1}{T_0}[\dot{m}_{exh}\left(1-\eta_{th,SG}\right)(h_c - h_d)] + \dot{m}_{exh}\left(1-\eta_{th,SG}\right)[s(T_d,P_{cc}) - s(T_c,P_{cc})]$$

The enthalpy h_c is estimated from the balance:

$$\dot{m}_{exh}\eta_{th,SG}(h_a - h_c) = \dot{m}_w[(h_7 - h_5)]$$

The temperature T_c and the entropies are estimated with the advanced equations of state as before.

5.3.6 Evaporator

The losses can be estimated as:

$$\Delta\dot{S}_{irr,EVA} = \frac{\dot{Q}_{diss,EVA}}{T_0} + \dot{m}_{exh}\left(1-\eta_{th,SG}\right)[s(T_b,P_{cc}) - s(T_a,P_{cc})] =$$

$$= \frac{1}{T_0}[\dot{m}_{exh}\left(1-\eta_{th,SG}\right)(h_a - h_b)] + \dot{m}_{exh}\left(1-\eta_{th,SG}\right)[s(T_b,P_{cc}) - s(T_a,P_{cc})]$$

The enthalpy h_a is calculated from the balance:

$$\dot{m}_{exh}\eta_{th,SG}(h(TOT_{CC}) - h_a) = \dot{m}_w[(h_8 - h_7)]$$

The temperature T_a and the entropy $s(T_a,P_{cc})$ are then estimated with the advanced equations of state. The enthalpy h_b and the entropy $s(T_b,P_{cc})$ are calculated using the advanced equations of state as before, but we need the temperature T_b which can be evaluated checking the TQ diagram as:

$$T_b = T_7 + \Delta T_{pp}$$

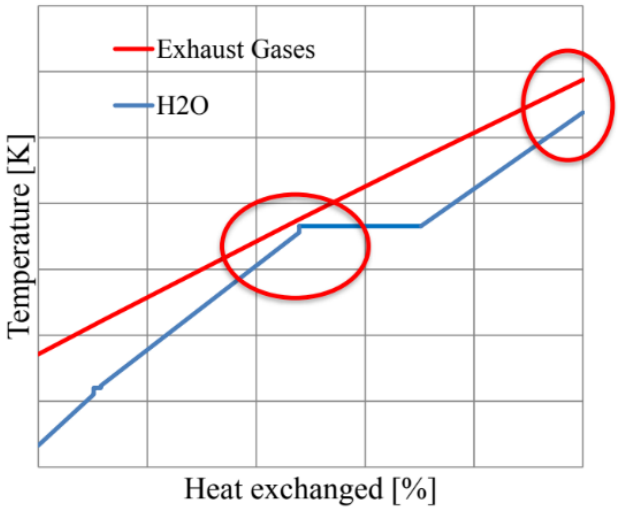

5.3.7 Superheater

The losses can be estimated as:

$$\Delta\dot{S}_{irr,SH} = \frac{\dot{Q}_{diss,SH}}{T_0} + \dot{m}_{exh}\left(1-\eta_{th,SG}\right)[s(T_a,P_{cc}) - s(TOT_{cc},P_{cc})] =$$

$$= \frac{1}{T_0}[\dot{m}_{exh}\left(1-\eta_{th,SG}\right)(h(TOT_{cc}) - h_a)] + \dot{m}_{exh}\left(1-\eta_{th,SG}\right)[s(T_a,P_{cc}) - s(TOT_{cc},P_{cc})]$$

5.8 Heat exchange losses between two fluids

These losses are due to finite temperature differences. Because of the ideal gas assumption, the distribution of pressure loss in HRSG can be only decoupled from heat exchange process.

5.8.1 Economizer for deaerator

The losses can be estimated as:

$$\Delta\dot{S}_{irr,ECO1} = \Delta\dot{S}_w + \Delta\dot{S}_{exh} + \Delta\dot{S}_{\Delta p,w,ECO1} =$$

$$= \dot{m}_w\left(s(T_3,P_3) - s(T_2,P_2)\right) + \dot{m}_{exh}\eta_{th,SG}\left(s(T_{stack},P_{cc}) - s(T_d,P_{cc})\right) + \Delta\dot{S}_{\Delta p,w,ECO1}$$

In the economizer the pressure losses on the water side which are equal to:

$$\Delta\dot{S}_{\Delta p,w,ECO1} = -\dot{m}_w\frac{v_3+v_2}{T_3+T_2}\Delta p_{ECO}$$

5.8.2 Deaerator

The losses can be estimated as:

$$\Delta\dot{S}_{irr,DEA} = \Delta\dot{S}_w + \Delta\dot{S}_{exh} =$$
$$= \dot{m}_w\left(s(T_4,P_4) - s(T_3,P_3)\right) + \dot{m}_{exh}\eta_{th,SG}\left(s(T_d,P_{cc}) - s(T_c,P_{cc})\right)$$

5.8.3 Economizer for steam generator

The losses can be estimated as:

$$\Delta\dot{S}_{irr,ECO2} = \Delta\dot{S}_w + \Delta\dot{S}_{exh} + \Delta\dot{S}_{\Delta p,w,ECO2} =$$
$$= \dot{m}_w\big(s(T_6,P_6) - s(T_5,P_5)\big) + \dot{m}_{exh}\eta_{th,SG}\big(s(T_c,P_{cc}) - s(T_b,P_{cc})\big) + \Delta\dot{S}_{\Delta p,w,ECO2}$$

In the economizer the pressure losses on the water side which are equal to:

$$\Delta\dot{S}_{\Delta p,w,ECO2} = -\dot{m}_w\frac{v_3 + v_2}{T_3 + T_2}\Delta p_{ECO}$$

5.8.4 Evaporator

$$\Delta\dot{S}_{irr,EVA} = \Delta\dot{S}_w + \Delta\dot{S}_{exh} =$$
$$= \dot{m}_w\big(s(T_7,P_7) - s(T_6,P_6)\big) + \dot{m}_{exh}\eta_{th,SG}\big(s(T_b,P_{cc}) - s(T_a,P_{cc})\big)$$

5.8.5 Superheater

$$\Delta\dot{S}_{irr,SH} = \Delta\dot{S}_w + \Delta\dot{S}_{exh} =$$
$$= \dot{m}_w\big(s(T_8,P_8) - s(T_7,P_7)\big) + \dot{m}_{exh}\eta_{th,SG}\big(s(T_a,P_{cc}) - s(TOT_{cc},P_{cc})\big)$$

5.9 HRSG pressure losses

The pressure losses of the HRSG can be estimated as:

$$\Delta\dot{S}_{irr,SH} = \dot{m}_{exh}R_g\ln\left(1 + \frac{\Delta p_{HRSG}}{p_0}\right)$$

5.10 Second law efficiency charts

The various trends of the second law efficiency losses can be visualized by the following diagrams. Such analysis is necessary to observe the effects of the operating pressure on the various processes.

Some considerations can be made:

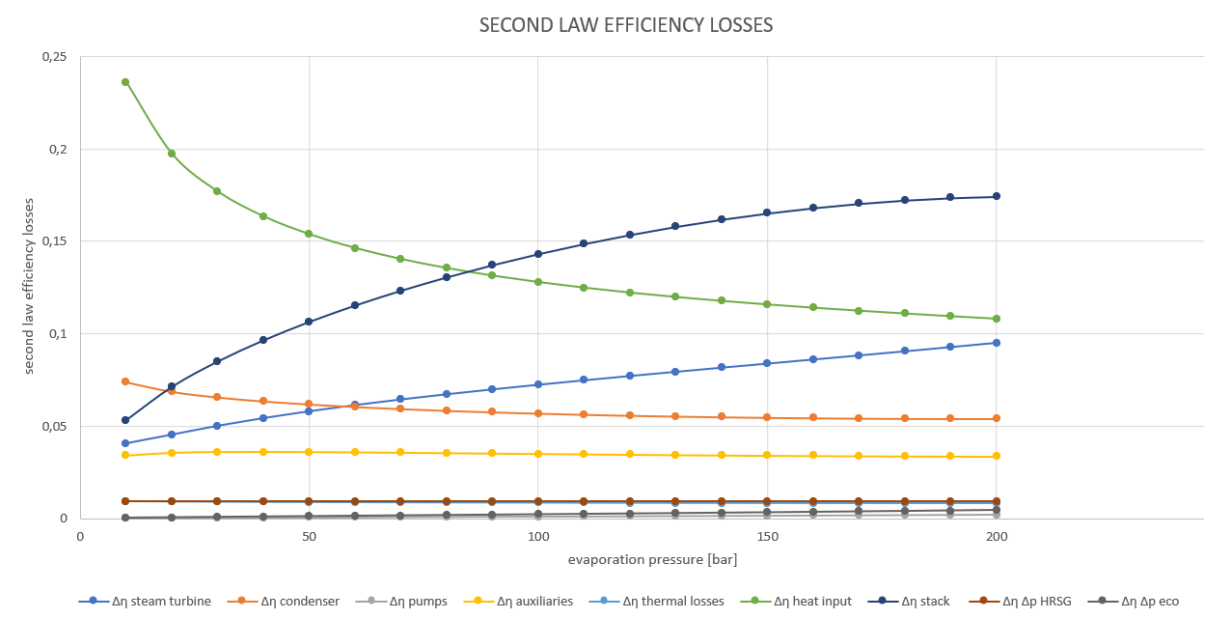

- The pumps' losses are very low and are directly proportional to the pressure difference.
- Increasing the evaporation pressure, the expansion ratio of the steam turbine increases.

- The evaporation pressure has a modest influence on the efficiency loss caused by the heat exchange with the ambient since the mass of water circulating in the cycle reduces and bi-phase fluid title at the turbine outlet decreases, which means that the heat that has to be extracted to obtain the saturated liquid is lower.
- The exhaust gases losses are directly proportional to the evaporation pressure because when this increases the stack temperature increases.
- The evaporator losses decreases because the evaporation temperature become closer to the exhaust temperature as the evaporation pressure increases; this behavior holds also for the superheater.
- The heat exchanged in the liquid form increases when the evaporation pressure increases so the economizer losses have a growing trend.
- The pressure losses of the economizers grow with the increasing of the evaporation pressure, but they are very little.
- The HRSG pressure losses don't change because Δp_{HRSG} doesn't vary.
- The optimal pressure which maximizes the net electrical power, corresponds to the highest second-law efficiency. This is because the optimal pressure is a trade-off between the steam generator efficiency losses which decrease as the evaporation temperature increases and the cost of expansion and pumping which increases as the evaporation temperature increases.
- The heat introduction inside the steam cycle decreases and so does the entropy generation relate to that process. Since the heat input at section cc is the same, decreasing the heat introduction in the cycle the heat rejection at the stack decreases.
- The auxiliaries' losses remain constant.

The following charts represent the cumulative second law losses:

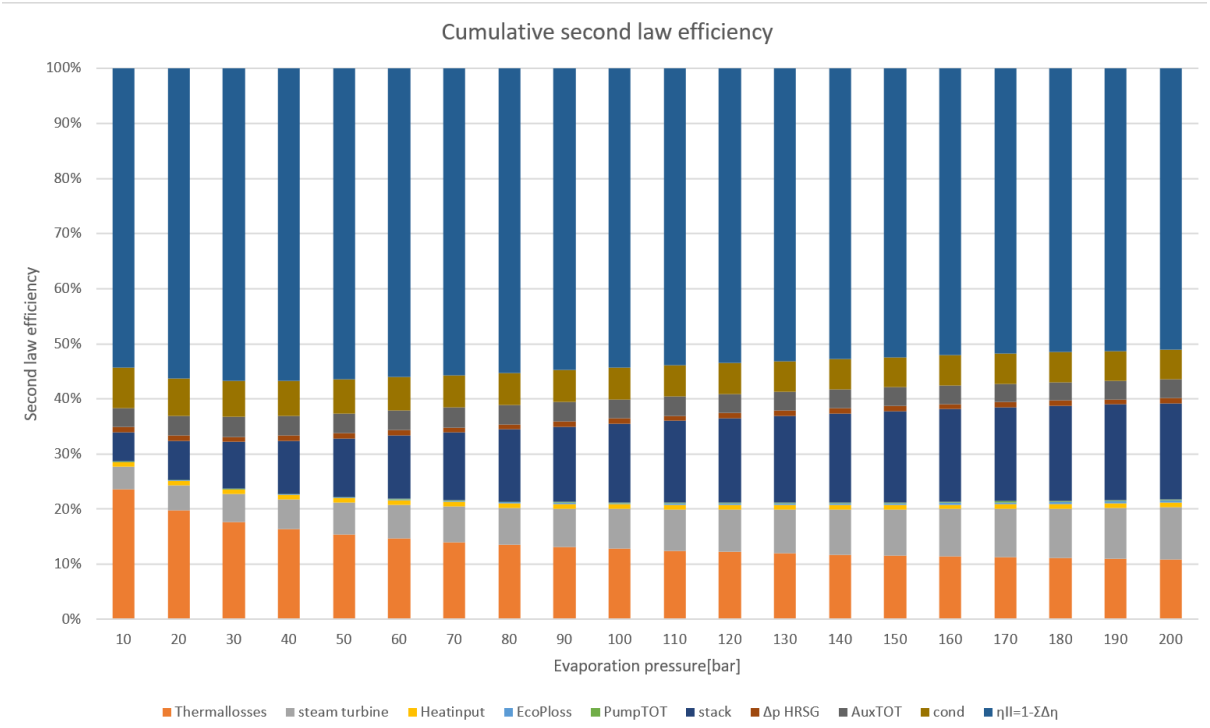

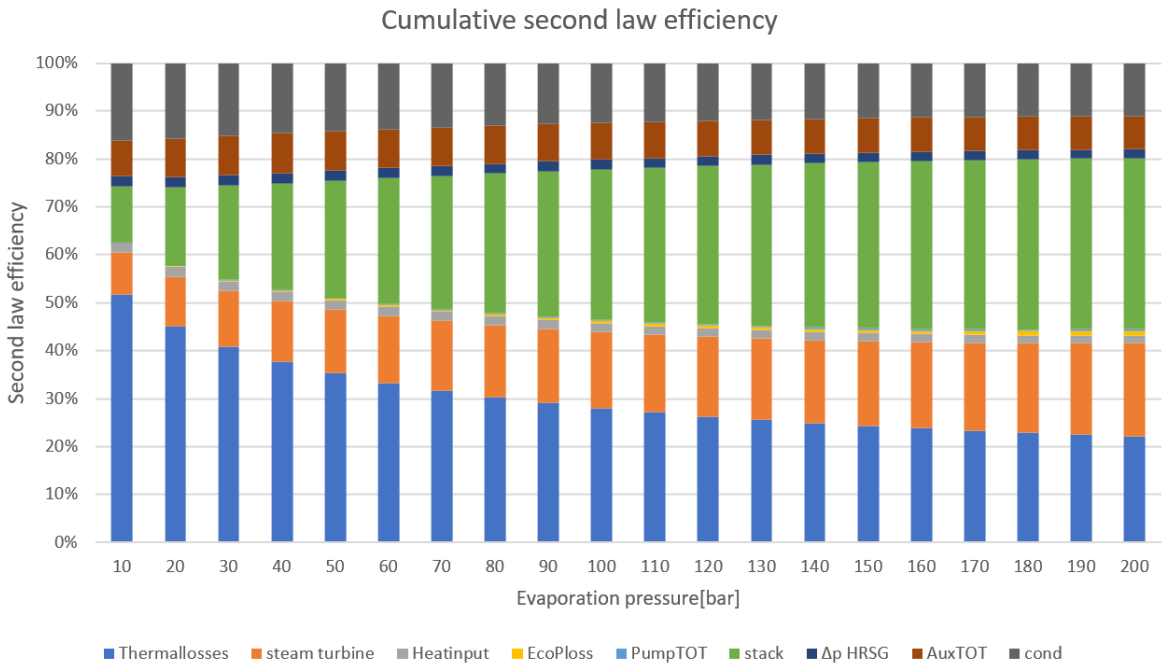
Cumulative second law efficiency
Second law efficiency
100%
90%
80%
70%
60%
50%
40%
30%
20%
10%
0%
10
20
30
40
50
60
70
80
90
100
110
120
130
140
150
160
170
180
190
200
Evaporation pressure[bar]
Thermallosses
steam turbine
Heatinput
EcoPloss
PumpTOT
stack
Δp HRSG
AuxTOT
cond

PROJECT 3
COMPARISON OF GAS TURBINE CYCLES

1.Introduction:

The aim of the document is to evaluate and compare the predicted performance of 4 different gas turbine cycles varying the most significant operating parameters. For each cycle, the performance is computed firstly form the first law efficiency point of view and then from the second law efficiency losses. In the last step, only for one cycle, its efficiency is analysed by individually modifying one of these three parameters: maximum blade wall temperature, turbomachinery performance and the filter and silencer presence.

To be noted that all the simulations are run with the aid of the software "*Turbogas*".

2.Data:

Gas Turbines Cycles

Simple gas turbine

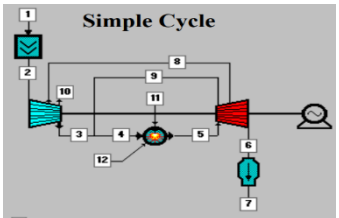

Intercooled gas turbine (IC)

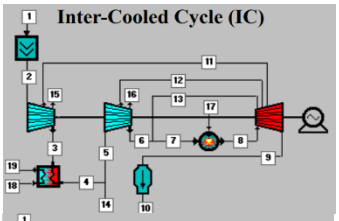

Recuperated gas turbine

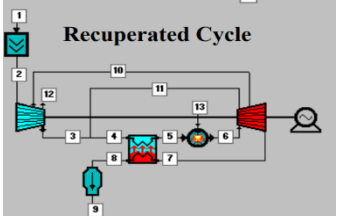

Intercooled – recuperative gas turbine (ICR)

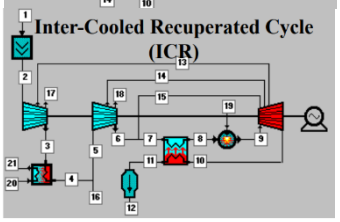

Ambient Conditions	Temperature: 15 °C
	Pressure: 1 atm
	Relative Humidity: 60%
Mass flow rate	Point 1: 121 kg/s
Inlet filter	Inlet pressure loss $\Delta p/p$: 1%
Compressor	Polytropic efficiency: η_{sp}: 0,905
	Organic efficiency: 0.997
	Leakage losses: 0,008 (only for HP compressor)
Intercooler	Hot side pressure loss $\Delta p/p$: 1%
	Air outlet temperature: 25°C
	Refrigerant water temperature: 15°C
	Thermal losses: 0%
Recuperator	Hot side pressure loss $\Delta p/p$: 2%
	Cold side pressure loss $\Delta p/p$: 2%
	Thermal losses: 0,7%
	Minimum ΔT at inlet/outlet: 25°C
Combustor	Combustion efficiency: 0,996%
	Pressure loss main stream $\Delta p/p$: 3%
Turbine	Maximum blading wall temperature: 800°C
	Film cooling effectiveness (parameter r_{fc}): 0.4

	Convective cooling effectiveness (parameter Z): 100
	Polytropic efficiency: η_{sp}: 0,89 (cooled stages)
	Polytropic efficiency: η_{sp}: 0,925 (uncooled stages)
	Organic efficiency: 0,997
Generator	Shaft rotating speed: 3000 rpm
Silencer	Outlet pressure loss $\Delta p/p$: 1%

Note: the values of some of the aforementioned parameters (mass flow rate, turbomachinery efficiencies, maximum blading wall temperature, blade cooling effectiveness parameters) have been calibrated in order to represent the simple cycle performance of large-size aero-derivative gas turbine engines (Power ≈ 40 MW, Efficiency ≈ 40%, at TIT = 1200°C and compression ratio β = 30)

3. First Law efficiency comparison

The following diagram shows the first law efficiency of each cycle as function of its specific work.

Each curve is sketched considering the following parameters:

- Total temperature at the turbine first rotor inlet equal to 1200°C.
- The pressure ratio β considered is within a range from 4 to 40. Except for the intercooled gas turbine cycle for which the maximum value of β is 90.
- For the intercooled gas turbine cycle, a β of the first compressor equal to $\beta_{LP} = \beta_{total}^{1/3}$ is taken.
- For the intercooled-recuperative gas turbine, a β of the first compressor equal to $\beta_{LP} = \beta_{total}^{1/2}$ is taken.

To be noted that the values of β are displayed on the chart.

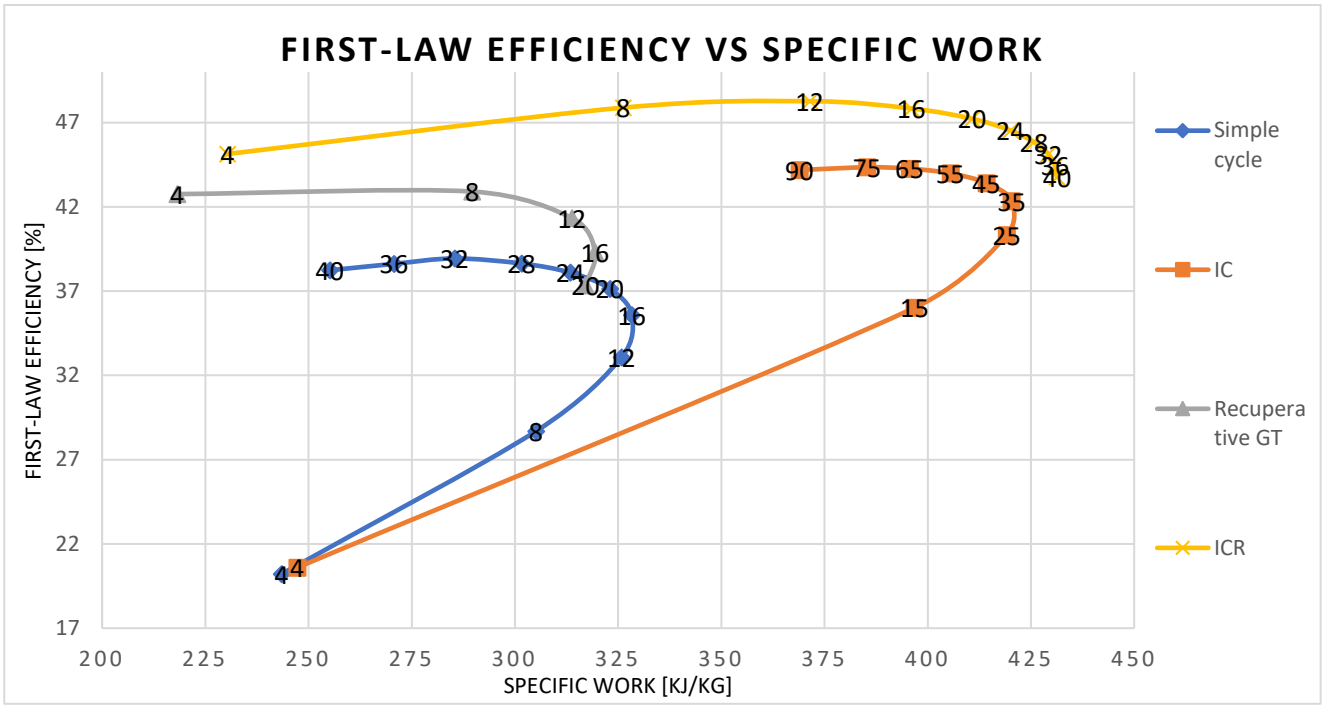

For each cycle, it can be observed as follows:

Simple Cycle (blue curve):	Both the efficiency and the specific work increase with the growing of β; up to β=16 for which the work reaches its maximum. Starting this point continuing to increase β, the specific work decreases, meanwhile, the efficiency grows up to stabilise for the higher values of β.
Intercooled Cycle (red curve):	The efficiency curve is quite similar to the simple cycle one. Therefore, the efficiency continues to grow along with β and the specific work reaches the maximum for intermediates values of β which are around 25-35.
Recuperative Cycle (green curve):	It is important underline that recuperative process imposes the following condition the temperature at the turbine outlet (TOT) > temperature at the compressor outlet (TOC) is met in order to happen, therefore β cannot be higher than 20. The efficiency curve has a different trend compared to the blue one. The specific work behaves in the same manner described above. It reaches the maximum values for β around 16 and then falls gentle. The efficiency remains stable up to β values about 10-12, and then decreases significantly. This behaviour is due to the decrease in difference between the TOT and TOC as β increasing, so the recovery is less effective.
Intercooled-Recuperative Cycle (purple curve):	As the previous cycle, the condition imposed by the recuperator should be met, therefore β cannot be higher than 40. In this case, the maximum pressure ratio is higher than the above cycle because it also considered the intercooled. The efficiency curve behaves as mixing of the two cases described above. Considering β grows: the efficiency increases up to β value about 15 and then pick down for the higher value of β and the specific work behaves like the other cases.

It is concluded that:

- The presence of intercooler allows to reach higher value of specific work due to the reduce work required to compressor to reach the outlet condition compared to the simple cycle. As the other parameters remain unchanged, the efficiency is higher to the simple one.

- The presence of recuperator allows to heat the fluid between the compressor and the turbine making less work than the simple cycle. Hence, for the range of β between 4 to 20, the recuperative cycle efficiency is clearly higher compared to the simple one.
- The intercooled- recuperative cycle takes advantage both the intercooler and recuperator. To be noted that the growing of the specific work is more evident compared to the IC because the first compressor pressure ratio is $\beta_{LP} = \beta_{total}^{1/2}$, while for the other cycle is $\beta_{LP} = \beta_{total}^{1/3}$. In this case, the performances obtained are the best of the four cycles analysed at the expense of the plant costs.

4. Second law efficiency comparison

For the second law efficiency analysis, the same parameters used for the first efficiency analysis are considered.

For each cycle, the sketch of the second-law efficiency losses computed via the entropy analysis as a function of beta is reported.

The losses evaluated are for:

- Combustion
- Compression
- Expansion
- Stack
- Recuperator
- Filter/silencer pressure losses
- Intercooling
- Various (mechanical and electrical losses)

4.1 Simple Cycle

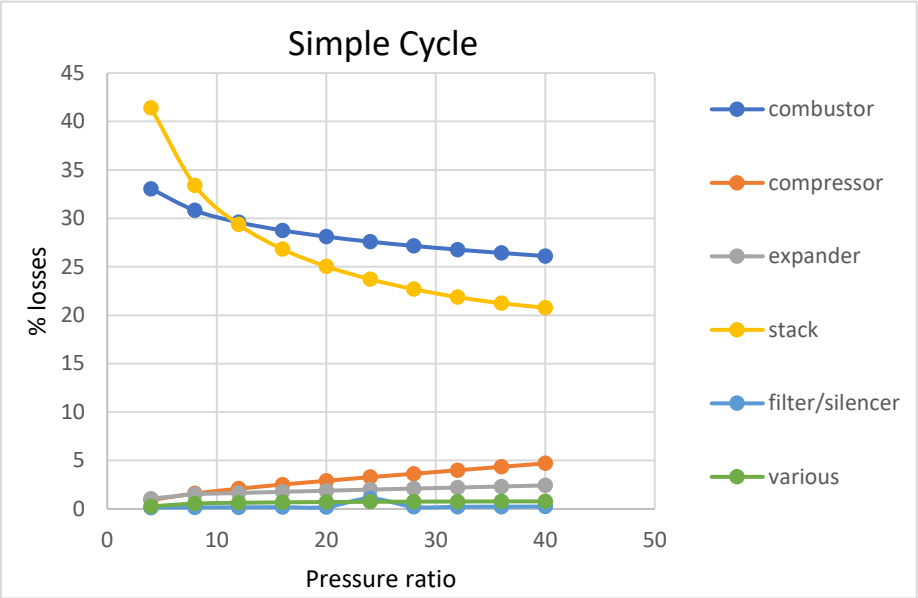

Observing the diagram, it can be deduced that:

- The two great losses are due to the combustion and the exhaust gasses. Both behave in an inversely proportional way with the trend of β. The losses fall with the increasing of β, starting from its maximum value at β=4.
  For the combustion, the trend of the losses is due the increase inlet combustor temperature caused by the compression ratio development. While for the exhaust gasses, the losses at the stack are influenced by two main factors: the increases of the fuel mass flow rate and the reduction of the outlet turbine temperature, both due to the growing of the β.
- The expander and the compressor losses behave proportionally to the trend of β. For both the higher value is appreciable at β=40
- The remaining losses due to the presence of filter/silencer and electromechanical power increases proportionally with the compression ratio. To be noted that, these losses are lower compared to the previous ones, therefore are neglected in this analysis.

4.2 Intercooled Cycle

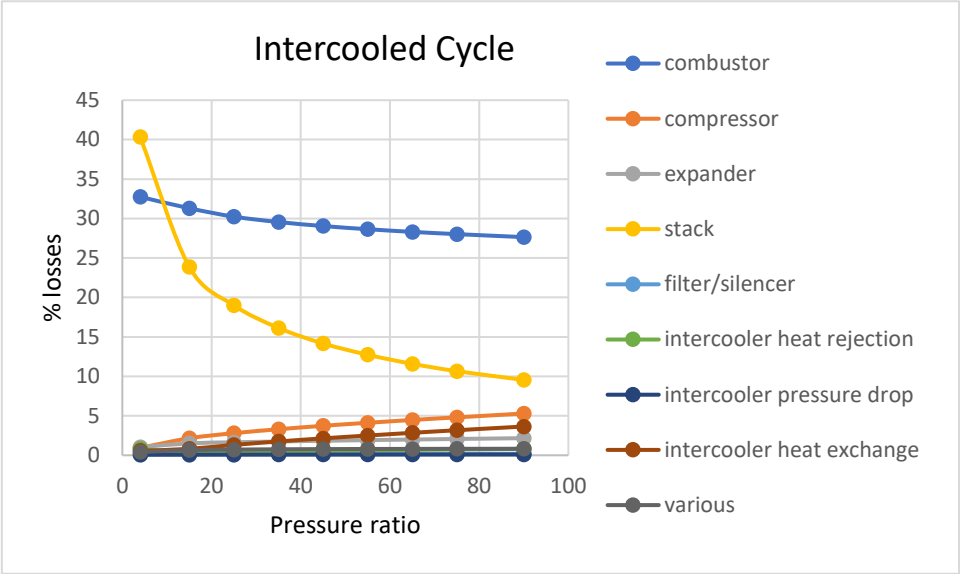

Observing the diagram, it can be deduced that:

- The intercooler installation does not influence the losses trend compared to the simple cycle. Therefore, all the consideration above reported, are also valid for this configuration.
  The two main contributions at the losses are due the stack and the combustor. Both behave in inversely proportional way to β. On the other hand, all the other losses are proportionally to the evolution of β.
- The presence of intercooler introduces three new losses to be considered: one due the pressure drops, and the other two caused by the thermal power. All behave in the same way of β, so their highest value is appreciable at β= 90. The losses are strictly linked to the fuel mass flow rate, which decreases with the β growing.
- To be noted that both the losses due the intercooler heat exchanger are negligible as their trend is quite constant in the range of β studied.

4.3 Recuperative Cycle

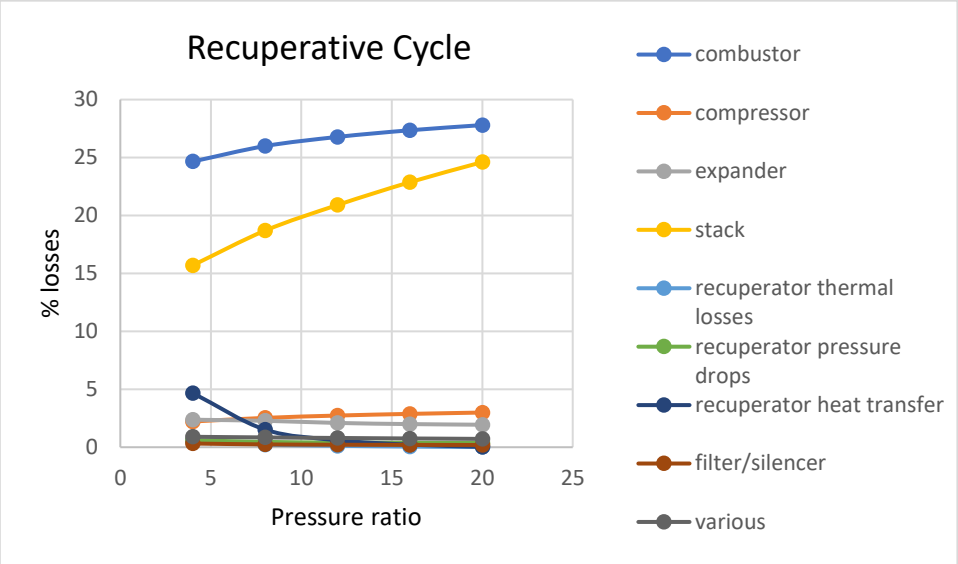

Observing the diagram, it can be deduced that:

- The presence of the recuperator influences the trend of the losses compared to the simple cycle analysed above. The most significant losses are due to the combustion and to the exhaust gasses. Both of them are directly proportional to the β evolution, which is completely opposite way respect the previous trend of these losses.
- For the combustion, the losses increase with the pressure ratio up to reach their maximum value at β = 20. This trends occurs because to continuously rising pressure ratio follows that the temperature difference between the inlet of turbine and the compressor outlet decreases. Consequently, the recovery heating power is lower, so it is necessary, that the working fluid is heated with more fuel.
- For the stack, the second law losses behave as the combustion one. This is due the fact that with the increasing of the pressure ratio, the temperature outlet of the compressor grows while the temperature at the outlet of the turbine drops down. This means that the temperature difference in the recovery is limited, and the temperature stack is higher.

4.4 Intercooled Recuperative Cycle

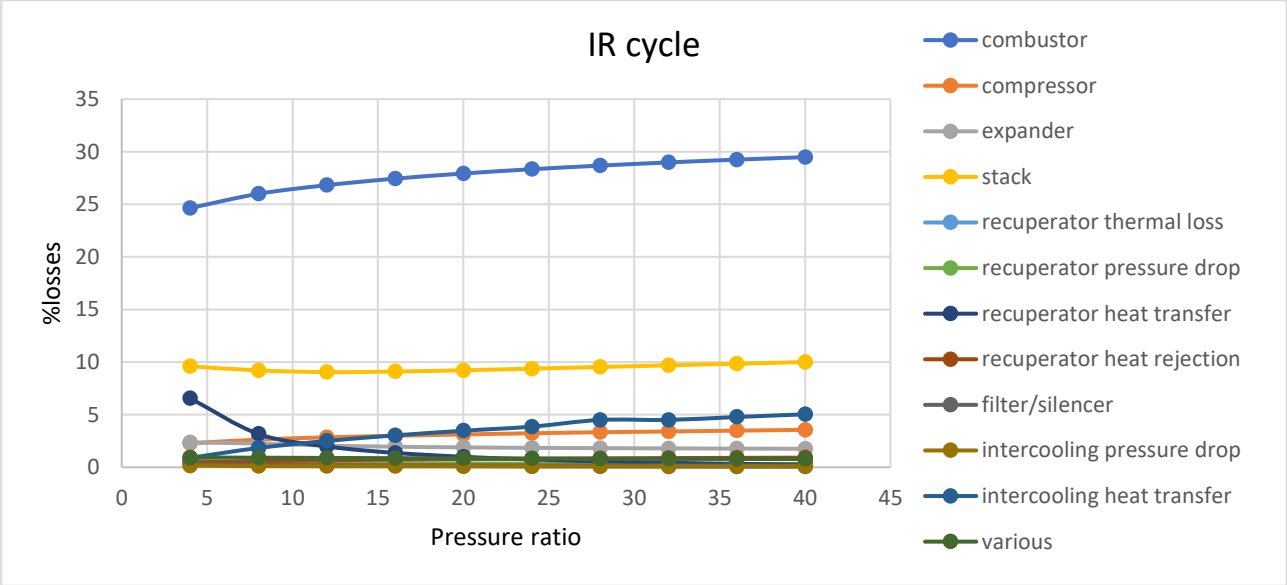

Observing the diagram, it can be deduced that:

- The installation of the intercooler and the recuperator simultaneously influences and combined the trend of the losses compared to the three cases described above.
- The most significant losses are due the combustion process. The losses are direct proportional with the pressure ratio. The reason of this behaviour is the same explained in the 4.3 paragraph.
- The stack losses are considerable reduced compared the previous one analysed. The path remains approximately constant thanks to the combined effect of recovery and intercooling.

4.5 Second Law Losses Comparison

The following two sketches summarize and compare the secondary losses of the four-cycle configurations analysed.

The cumulative losses are displayed:

- in a diagram to appreciate the different trends as a function of the pressure ratio;
- in a bar chart, to highlight how they vary according to the configurations for the best β value.

It is appreciable that the second law performance of the simple configuration is enhanced by the installation of both the recuperator and the intercooler. The only intercooler fitting allows to reach higher value of the β with an unprofitable of the totally losses. The only recuperator layout allows a significant reduction of the totally losses but at the expense of a limited pressure ratio range. To be noted that, for the highest efficiency cases, despite the consideration made above, the intercooled configuration is better than the recuperative one.

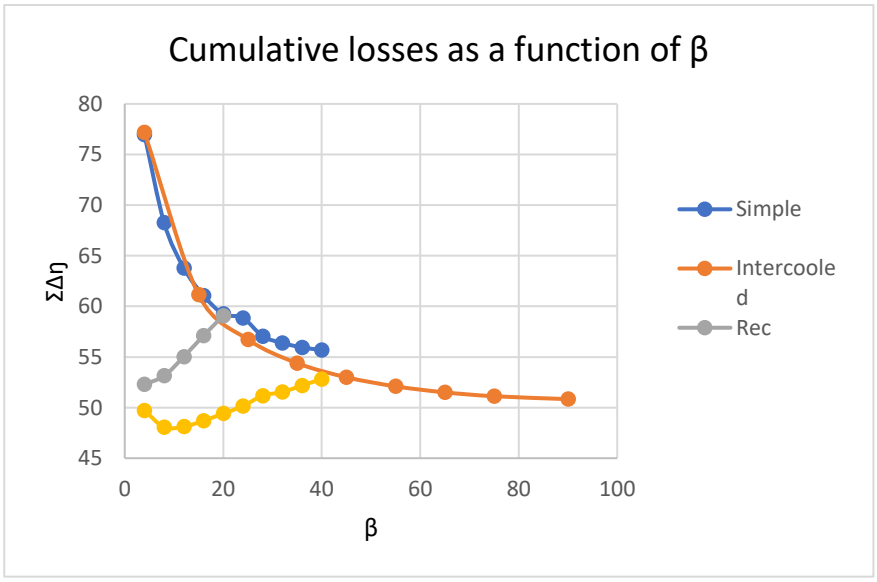

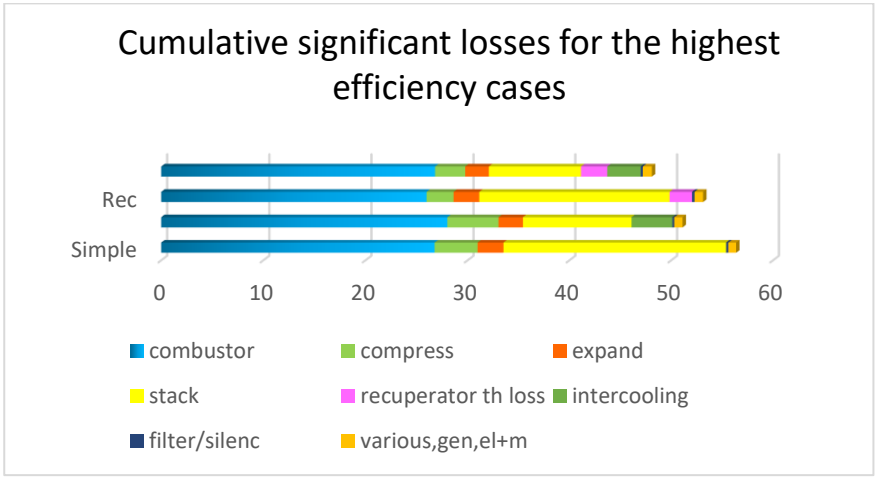

5. Sensibility of the first-law efficiency

Considering the simple cycle configuration at β = 32, which is the optimal value obtained from the first law efficiency prospective, the sensibility of the efficiency is analysed by individually modifying one of these three parameters: maximum blade wall temperature, turbomachinery performance and the filter and silencer presence.

5.1 Maximum blade wall temperature

The behaviour of first efficiency is analysed within a TIT range between 900°C to 1300°C, varying the T_{max} allowable by the blades. It means changing the blades materials and the presence or not of the cooling system.

Three cases are evaluated:

- $T_{max,blade,base} = 5000°C \quad Adiabatic\ system$
- $T_{max,blade} = T_{max,blade,base} + 100°C$
- $T_{max,blade} = T_{max,blade,base} + 300°C$

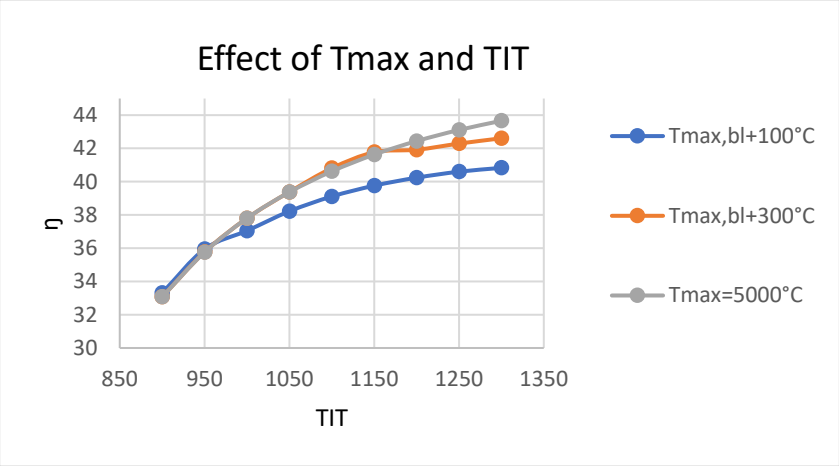

Looking at the diagram, it can be observed as follows:

- For $T_{max,blade,base} = 5000\ °C$, the efficiency increases as square root with the TIT growing. Apparently, no perturbations are present.
- For Tmax = Tmax,bl + 300 °C the efficiency behaviour is similar to the adiabatic one upon the 1150°C. Above this temperature, the efficiency increasing more gentle because the cooling system is activated.
- For Tmax = Tmax,bl + 100 °C the same considerations made for the second case can be applied also here. To be noted that the cooling process is activated at 950 °C.

In conclusion, cooling flow in the first turbine stages decreases the entropy of the initial expansive process, meanwhile the irreversibility of the system grows leading to the efficiency drop down.

5.2 Turbomachinery performance

The behaviour of first efficiency is analysed within the turbomachinery performance varying the polytropic efficiency both the compressor as the turbine between a range of [-0,3: +0,3].

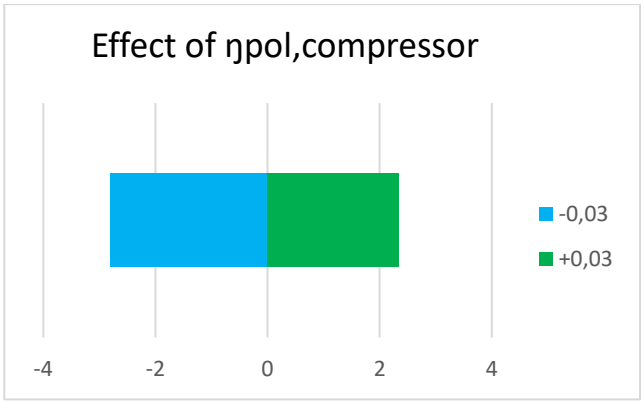

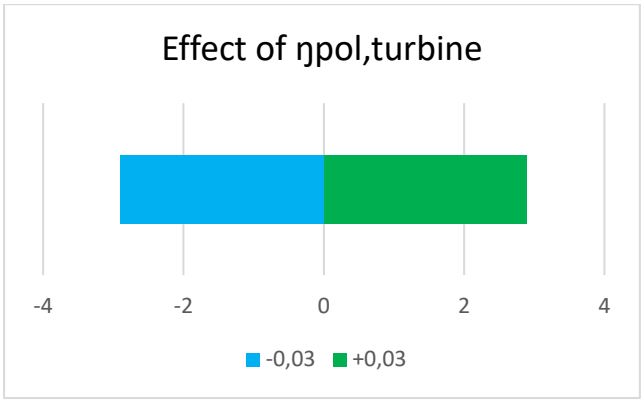

The major impact on the cycle efficiency is due to the turbine polytropic efficiency along all range. Infacts, the turbine work contribution is higher compared to the compressor one upon the cycle total work output. Consequently, the perturbation of its efficiency has a considerable larger impact upon the total one.

5.3 Filter and Silencer Pressure Losses

The behaviour of first efficiency is analysed within filter and silencer pressure losses increasing their nominal value of 10%.

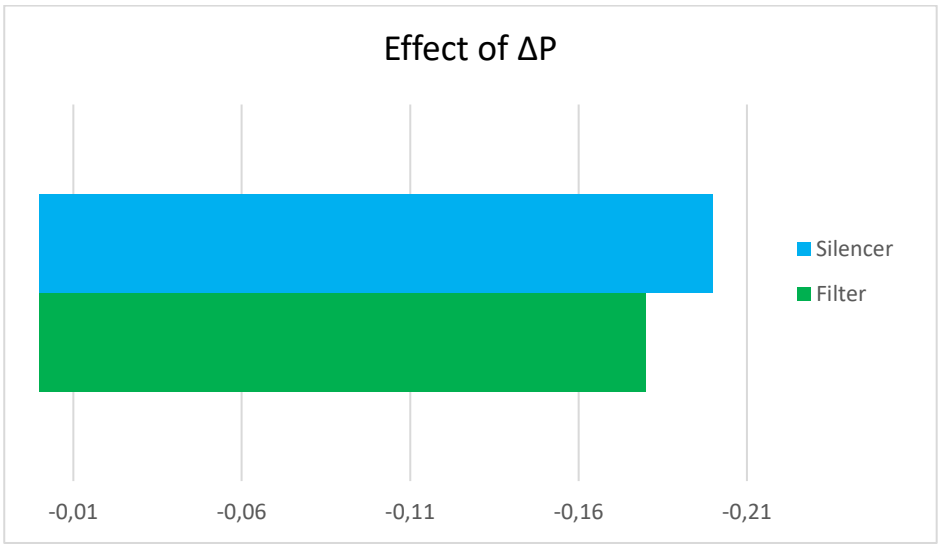

The pressure drops changing both in the silencer as in the filter leads to a reduction of the cycle efficiency.

PROJECT 4
ADVANCED STEAM CYCLES

1. Introduction:

The document aims to evaluate the performances of different fired steam Rankine cycle configurations via the use of the software CicVap.

The analysis is started considering an Ultra-Supercritical Cycle (USC) in a base configuration moving towards more complex and articulated layouts.

2.Data:

Configuration A

- Superheater outlet mass flow rate: 1˙850˙000 kg/h
- Superheater outlet steam pressure: 270 bar
- n° reheaters: 1
- n° preheaters (deaerator included) : 8 (4 LP, 4 HP)
- n° mid-pressure two-flow rotors: 1
- n° low-pressure two-flow rotors: 2
- last stage blading: 33.5 inches – mean diameter 99.5 inches
- steam temperatures: 580°C / 580°C
- condensing pressure: 0.05 bar
- fuel: coal
- exhaust gas stack temperature 150°C
- O2 concentration in exhaust gases at the stack: 5%
- economizer water inlet temperature: approx. 315 °C

The alternative configurations that are different from configuration A by the mentioned characteristics:

Configuration B: - fuel: natural gas
- exhaust gas stack temperature: 120 °C
- stack O2 concentration in exhausts: 2.5%

Configuration C: - condensing pressure: 0.1 bar

Configuration D: - steam temperatures: 640°C / 640°C

Configuration E: - n° preheaters: 4 (2 LP deaereator included, 2 HP)
- economizer water inlet temperature: ~ 280 °C

Configuration F: - n° re-heaters: 2
- steam temperatures: 580°C/580°C/580°C

3. Analysis:

The performance of each cycle can be evaluated from two point of views based on:

- The first law efficiency prospective
- The entropy analysis which considers the second law efficiency losses

For this investigation, the outlook setting for the first law efficiency is reported only for the configuration A while the second law analysis is estimated for all layouts.

3.1 First Law Analysis:

Firstly, the plant scheme is shown below. The scheme neatly highlights the 8 preheaters (4 LP + 4HP), the SH and RH mechanism and the multiple stage steam turbine that characterize the system. The bleeding lines are clearly visible, running mainly from the turbines (either HPT or LPT) to the preheaters and then back into the cycle after the condenser to guarantee a constant working liquid mass flow. The presence of a small Dedicated Steam Turbine (DST) can be noticed as well, having the only task to provide persistent power output to the feed water pump positioned after the deaerator. The temperature and pressure of the main streams at the turbines inlet and outlet are underlined in red alongside the chart.

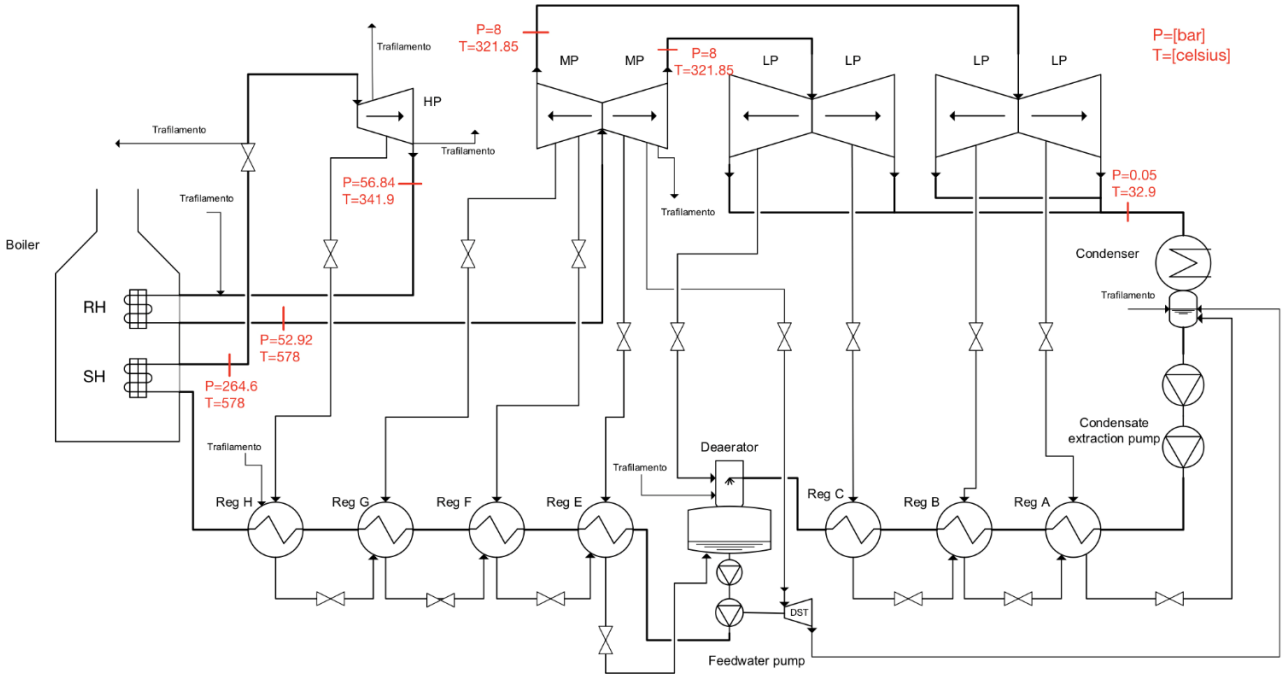

The first law analysis for the cycle, above described, can be easily appreciated by the Sankey Diagram, as follows:

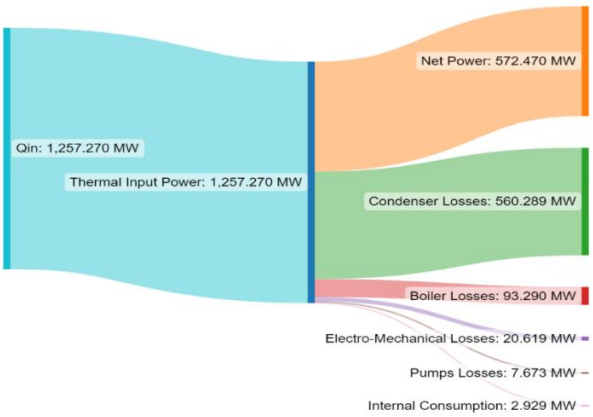

The diagram shows that:

- The net power output sits at 572.47 MW with a thermal input of around 1.26 GW.
- The largest loss takes place in the condenser, which accounts to around 45% just by itself.
- The remaining losses notable of value are the one in the boiler (7.4%) and in the turbine (a.k.a. electro-mechanical, 1.65%).

The obtained values are in line within the expected for an ultra supercritical power plant.

For completeness, in this section, the secondary losses of the configuration A are shown below by a Sankey Diagram. The diagram is the result of a careful grouping of the values given by the entropy analysis carried out, as listed in the next section.

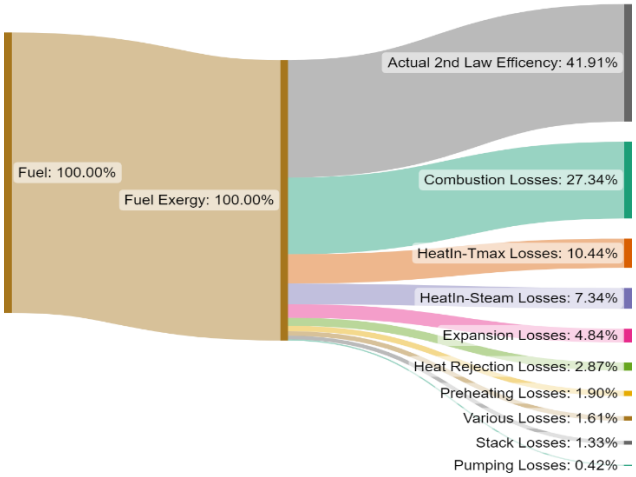

Being conceptually different from the 1st law analysis, the biggest loss develops in the combustion (27%) followed by the heat input losses, furthermore, divided into steam and T_{max} cases. The condenser losses become significantly less influential. The reason is due to the fact that the power exchange in the condenser is relatively high while the condenser temperature is in proximity of the dead state.

3.2 Second Law Analysis:

For all configuration, the entropy analysis is reported grouping the second-law efficiency losses as follows:

- combustion loss (including air as well as fuel pre-heating);
- cycle heat introduction loss: heat exchange between exhausts and isothermal line at T_{max} ;
- cycle heat introduction loss: heat exchange between isothermal line at T_{max} – steam;
- preheating loss (deaerator included);
- cycle heat rejection loss;
- working fluid pumping loss;
- working fluid expansion loss (including outlet kinetic energy loss);
- stack loss;
- various losses.

The obtained results by the CicVap are summarised and easily visualised in the table and in the bar chart below reported.

Losses	Config A	Config B	Config C	Config D	Config E	Config F
Combustion	27.34%	26.27%	27.34%	27.28%	28.11%	27.37%
Heat introduction to Tmax	10.44%	11.58%	10.44%	8.46%	9.68%	10.42%
Heat introduction to steam	7.34%	7.40%	7.34%	8.26%	7.95%	6.87%
Preheating	1.90%	1.91%	1.81%	1.98%	2.01%	1.46%
Heat rejection	2.87%	2.89%	4.83%	2.79%	2.91%	2.77%
Pumping	0.42%	0.42%	0.41%	0.39%	0.37%	0.42%
Expansion	4.84%	4.88%	4.35%	4.63%	4.95%	4.32%
Stack	1.33%	0.75%	1.33%	1.33%	1.33%	1.33%
Various	1.61%	1.62%	1.59%	1.63%	1.60%	1.63%
Cumulated losses	58.09%	57.74%	59.45%	56.74%	58.91%	56.58%
2nd law efficency	41.91%	42.26%	40.55%	43.26%	41.09%	43.42%

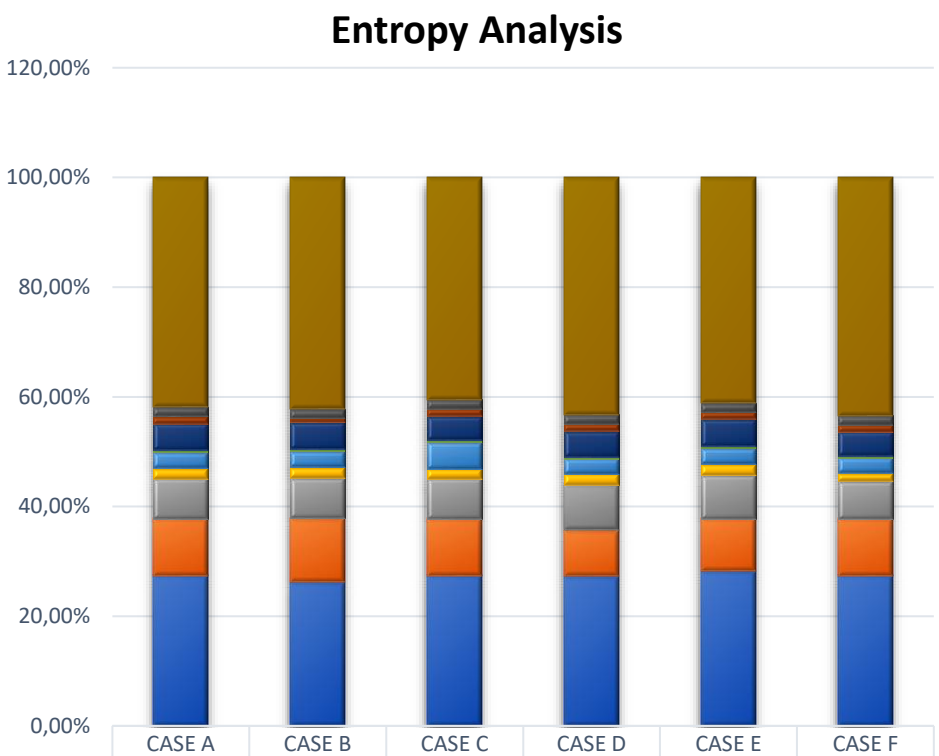

	CASE A	CASE B	CASE C	CASE D	CASE E	CASE F
2nd Law Efficency	41,91%	42,26%	40,55%	43,26%	41,09%	43,42%
Various	1,61%	1,62%	1,59%	1,63%	1,60%	1,63%
Stack	1,33%	0,75%	1,33%	1,33%	1,33%	1,33%
Expansion	4,84%	4,88%	4,35%	4,63%	4,95%	4,32%
Pumping	0,42%	0,42%	0,41%	0,39%	0,37%	0,42%
Heat rejection	2,87%	2,89%	4,83%	2,79%	2,91%	2,77%
Preheating	1,90%	1,91%	1,81%	1,98%	2,01%	1,46%
Heat introduction to steam	7,34%	7,40%	7,34%	8,26%	7,95%	6,87%
Heat introduction to Tmax	10,44%	11,58%	10,44%	8,46%	9,68%	10,42%
Combustion	27,34%	26,27%	27,34%	27,28%	28,11%	27,37%

For each configuration a comparison with the A one is reported:

Configuration B Considering the natural gas as fuel, the combustion losses decreases because the NG has a heating value higher compared to the coal. Therefore, the air needs a lower preheating. The stack losses gets gently down because the outlet temperature is lower. The total efficiency increases little.

Configuration C The irreversibility in the condenser grows due to the increases of the pressure and temperature of condensation. The pressure ratio reduces and consequently the losses in the turbine drop. This reduction results not enough to compensate the condenser one. Therefore, the efficiency is worse.

Configuration D

The raise of the steam temperature generates two effects:

- The ΔT of the heat transfer between the exhausts and the T_{max} goes down and together with its irreversibility.
- The mean log temperature increases and consequently its ΔT of the heat transfer with the T_{max} grows. Therefore, the losses increase.

The total losses due to the heat introduction in the cycle slow significantly down allowing a net improvement of the efficiency.

Configuration E The reduction of the preheaters leads a significantly grow in the heat transfer losses. In fact, the water gets into the economizer with a lower temperature, therefore the heat to reach the maximum temperature increase. The efficiency is considerably lower.

Configuration F The introduction of more preheating leads to a decrease of the losses due to the heat transfer. The total efficiency is significantly higher.

In conclusion, the two possible solutions to improve the second law efficiency are the following:

1) Increase of the steam temperature, considering the withstand limits of the material.
2) Increase the number of preheating to have higher steam mid temperature which absorbs heat.

PROJECT 5
ANALYSIS OF AN AXIAL FLOW EXPANDER

1. Introduction:

The aim of the document is the determination of stage operating conditions and geometric parameters of an uncolled expander by means of an axial-flow turbine design and optimization tool.

Three configurations are analysed:

- Three-stage machine
- Two-stage machine
- Single-stage machine

Firstly, the stage efficiency of each configuration is evaluated and then compared.
In the second step, considering only the first stage of the three-stage machine configuration, a sensitive analysis on rotational speed within the range [5000-25000 rpm] is performed and then the optimal value of rotational speed that allows for maximum efficiency is determined.
To be noted that all the analysis are computed by the Axture Software.

2. Data:

Mass flow rate:	10 [kg/s]		
Inlet total pressure:	5 [bar]		
Inlet total temperature:	850 [C°]		
Working fluid property:	Ideal gas	MM = 30	γ = 1.31 – 1.35
Rotational speed base cases:	10000 [RPM]		
Maximum peripheral speed:	$\approx$350 [m/s]		

3. Stage efficiency evaluation:

For each configuration, the stage efficiency is evaluated considering a fixed rotational speed at 10000 rpm.
In the analysis the following parameters are compared:

- Isentropic head coefficient
- Stage reaction coefficient
- Isentropic enthalpies drop
- Stage inlet and outlet total temperatures
- Velocity triangles, and geometries losses

3.1 Results and comments

3.1.1 Efficiency and stage parameters

The following table summarized all the evaluated parameters with respect of each stage for all configurations.

	Three-stage machine			Two-stage machine		Single stage machine
	1° Stage	**2° stage**	**3° stage**	**1° Stage**	**2° stage**	**1° Stage**
η_{global} [%]	92	92	92	91	91	87
K_{is} [-]	3.07524	2.80304	2.30436	3.01047	2.51059	2.78452
r*[-]	0.42674	0.46593	0.46197	0.41587	0.42852	0.39771
Δh_{is} [J/kg]	159012.5	147850.8	123990.4	229621.4	195342.4	414790.1
T_{totin} [K]	1123.15	1002	888	1123.15	948	1123.15
T_{totout} [K]	997	883	788	943	792	801

a) **Three stage machine:** This configuration reaches the highest value of efficiency for all stages: 92%.
The kinetic energy at the discharge will be lower compared to the other configurations because the outlet stage temperature is the lower one.
The stage reaction coefficient is about 0.5, optimal value for a reaction stage. The values obtained for the K_{is} are in line within the expected one for a reaction stage. Therefore, the lower K_{is} values obtained generate a little isentropic enthalpy jump.

b) **Two stage machine:** This configuration has lower value of efficiency compared to the previous case without a complete collapse of performances. The performances losses are linked to the lower value of r*. The r* values is around to 0.4, therefore the associated load coefficient is higher. The temperature differences between the outlet and the discharge is grown as well the kinetic energy.

c) **Single stage machine:** This configuration corresponds to a complete impulse turbine. The single stage has to exploit the whole enthalpy drop. Actually, it is characterized by the lowest reaction degree and the highest load coefficient. The efficiency decreases significantly until the 82%.

Analytically, the stage load coefficient and the reaction degree can be calculated as follows:

$$\begin{cases} K_{is} = \dfrac{\Delta h_{is}^{stadio}}{u^2/2} \\ r* = \dfrac{\Delta h_{rotor}}{\Delta h_{stage}} \end{cases}$$

It may be concluded that the isentropic loading goes up within a smaller degree of reaction as the stage needs to manage an higher enthalpy drop. Therefore, the efficiency goes lower within a smaller and cheaper machine.

3.1.2 Velocities triangles and geometries losses

The velocities triangles of each stage for all configurations are under reported highlighting the geometries losses related.

THREE-STAGE MACHINE

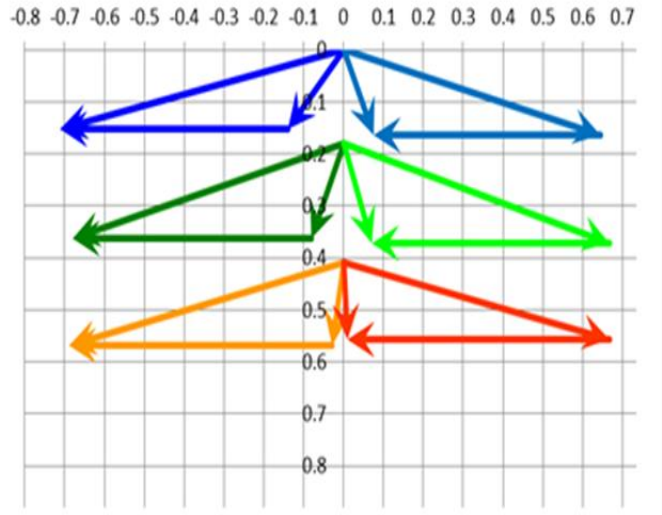

From the parameters analysis of the machine, this configuration has three stages similar to 0.5 reaction stage. The velocity triangle in blue differs little from the 0.5 reaction stage. It is appreciable that the axial velocity at the outlet is slightly increasing. It means that the stage behaves like a nozzle.
Both the second stage velocity triangle which is in green colour as the last stage velocity triangle, in red colour, are near the 0.5 reaction degree one. Only the last stage is optimized (V_{out} is around zero). It is also appreciable that the axial velocity at the outlet is slightly decreasing, so the stage behaves like a diffuser.

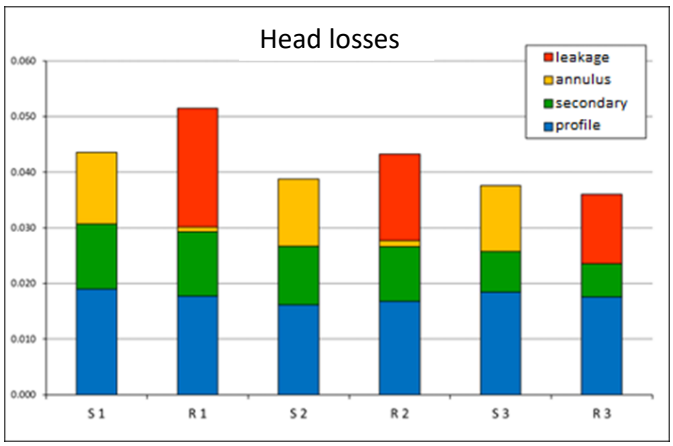

The graph summarized all the head losses in the machine. The profile losses, linked to the shape of the blade, along all the stator and rotor are almost constant. The secondary losses are slightly decreasing along all stages because the cross-section areas of the channels are increasing along all the machine, reducing the impact of the vortexes and the phenomena like that on the flow. The losses in the annuluses are significant only in the stators because they are still components. On the other hand, the leakage losses are more significant in the rotor where the mechanical work exchange with the fluid happens.

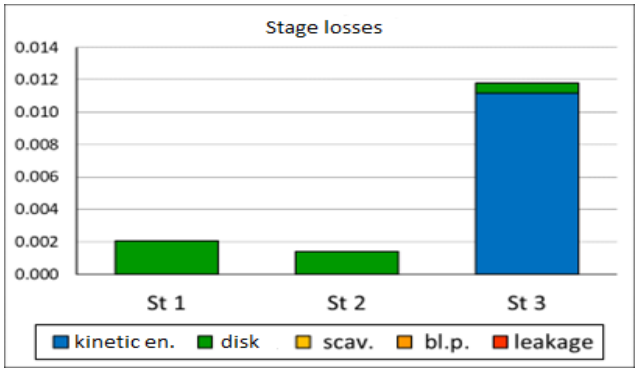

The following graph summarized the stage losses. Disk losses are more significant in the first stages because the fluid is pressurized, and the channels are tighter. The kinetic energy losses are concentrated at the end of the last stage.

TWO-STAGE MACHINE

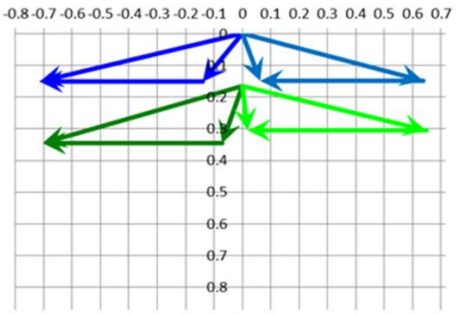

The velocity triangle of the first stage is similar to the one of the three-stage machine.
In fact, its r* value is quite near to 0.5
The axial velocity of the of the second stage is appreciable lower. This is due the presence of diffusion inside the rotor to minimise the kinetic energy loss at the outlet of the machine.

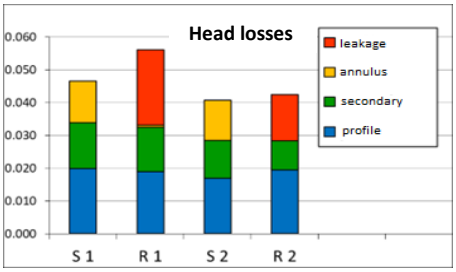

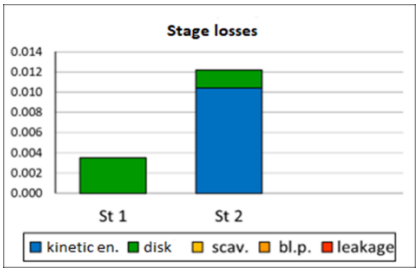

Both the head losses as the stage losses trends are similar to the three-stage one.

SINGLE STAGE MACHINE

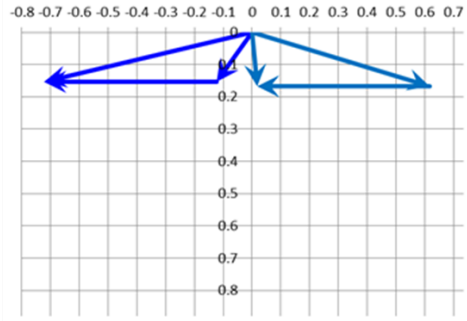

The velocity triangle of the single stage is near to the optimized conditions as the tangential absolute velocity at the outlet of the rotor is not exactly 0.

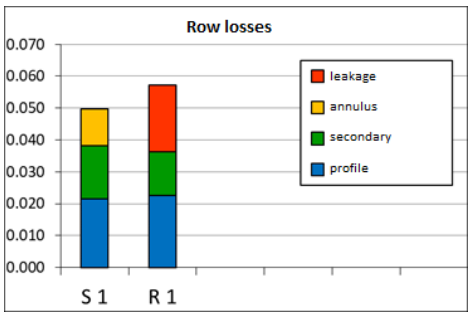

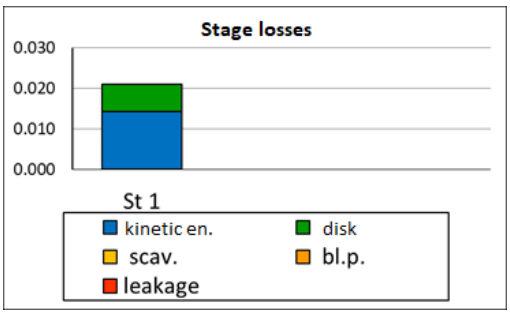

The trend of head losses and stage losses are similar to the previous case.

4. Sensitive analysis

The sensitive analysis is performed for the first stage of the three-stage machine in order to underline the trend of the turbine parameters within a range of the rotational speed from 5000 to 25000 rpm.

The variables of interest are the overall efficiency, the specific rotational speed, the mean value of the h/D ratio both for the stator and for the rotor, and the machine losses (profile, secondary, annulus, leakage both for stator and for rotor, kinetic energy and disk).

Performing the simulations with the default input parameters of the simulation tool and with the given operating conditions the following problems for some values of the rotational speed are found:

- from 13000 to 14000 rpm, it is necessary increase the flare tip and flare hub limits respectively from 30° and -30° to 32° and -32°
- from 15000 to 16000 rpm, it is necessary increase the h/D limit from 0.3 to .5
- from 16000 to 17000 rpm, it is necessary increase the flare tip and flare hub limits respectively from 32° and -32° to 34° and -34°
- from 19000 to 20000 rpm, it is necessary increase the h/D limit from 0.5 to 0.7
- over 21000 rpm, no way to go was founded.

The changes in the flaring angles limits and in the h/D limit are due to the fact that increasing the speed, the machine (in the simulation) becomes smaller not to exceed the critical peripheral velocity related to the material resistance. A smaller machine has a lower mean diameter so a higher h/D by default; furthermore, at the same inlet mass flow rate, it is more stressed on the volume flow rate increase along the axial direction of the flow, so it requires higher blades with respect to the mean diameter and higher flaring angles in the last stages. A possible clarification of no solution founded beyond 21000 rpm is that at higher rotational speeds it's impossible to combine together the limits on the h-d ratio and on the flaring angles with the limit on the peripheral velocity. More precisely, the ratio between blade height and mean diameter should never exceed 0.3. For higher values, sub-optimal conditions are found given that the spacing at the tip of the blade increases a lot, with the need to also increase the chord in order to maintain the best geometric ratio b/s. During the simulations the latter parameter was not adjust, probably incurring in an impossible numerical problem solution. If b/s changes, however, it would have been the exact opposite of what is required by the stress limitation on blade row that requires tapered blades, and therefore, an unavoidable disadvantage on efficiency. Another fact that makes high speeds critical is that in the event of flaring angles greater than 30°, the radial component of velocity starts to be a disadvantage and it is always good to remain below this threshold. Probably the fact of being above 30° of flaring angles in the simulations has been a contribute to the errors in running the software.
In conclusion, the best efficiencies at very high rotational speeds cannot be calculated.
The plots of the trends of the parameters are reported below.

4.1 Parameters trend

4.1.1 Efficiency

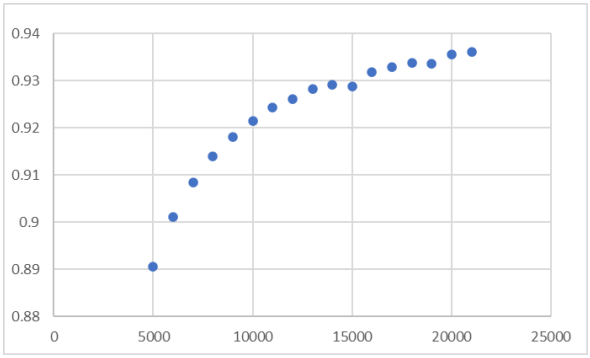

The trend of the efficiency seems to be a composition of three downward concavity parabolic curves. The changes in the curve occur at 16000 rpm and 20000 rpm, namely the critical steps point when the h/D ratio was increased to manage the speed.
The absolute maximum efficiency of the investigation is 93.6% at rotational speed around 21000 rpm. While the maximum efficiency without changing the limit on the h/D ratio seems to be around 14000 rpm (eta = 92.9%). Remembering the considerations made before regarding the management of the limits at high rotational speeds, the considered result as the most meaningful.

4.1.2 Specific rotational speed

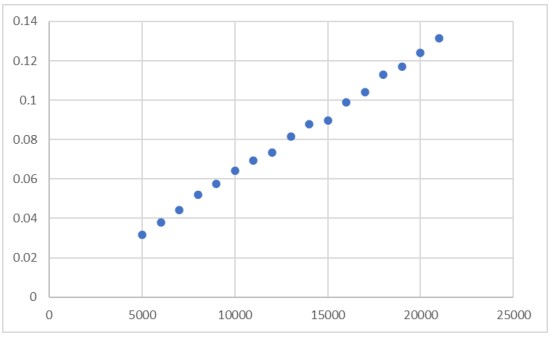

The trend of Ns is almost linear, and this is consistent with its definition:

$$N_s = N \frac{\sqrt{\dot{V}}}{(\Delta h_{stage})^{0.75}}$$

where the volume flow rate and the enthalpic drop of the stage are almost constant with the rotational speed.
At N_{opt} = 14000 rpm found before the N_{s_opt} = 0.088. It is around the optimal value 0.1 from literature.

4.1.3 Blade height-diameter ratio

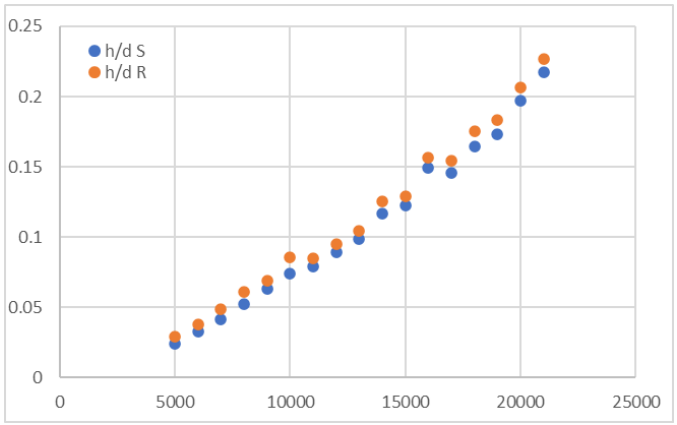

The h/D ratio increases proportionally with the rotational speed. Form the similarity theory, it possible says that: high rpms correspond always to small machines, and the viceversa. So, at higher rpms the software will return a smaller machine, and a bigger one for small rotational speeds. On the other hand, the blade height does not change much, just what is needed to compensate the diameter increase and guarantee that the same mass flow rate is discharged.

4.1.4 Profile losses

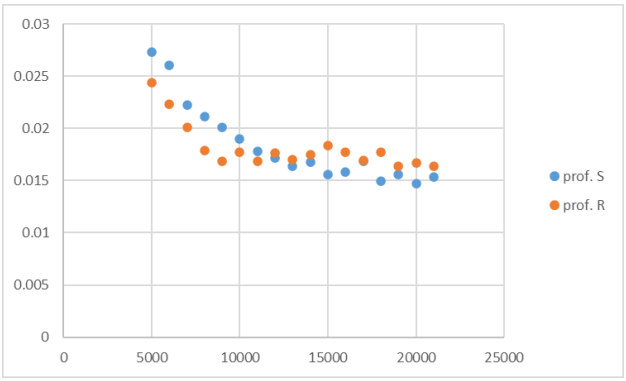

It is appreciable that the rotor and the stator have almost the same behaviour. This is since the degree of reaction is around 0.5 for any rotational speed, and hence both rotor and stator show a similar geometry and a similar loading. The minimum of the losses is found around the optimal rotational speed. Here as before made for the efficiency, it is necessary distinguish an absolute optimum point (that considers the changes in h/D) and a “relative” one (without changing h/D). So again, the two minimum points are respectively around 19000 rpm and 14000 rpm.

4.1.5 Secondary losses

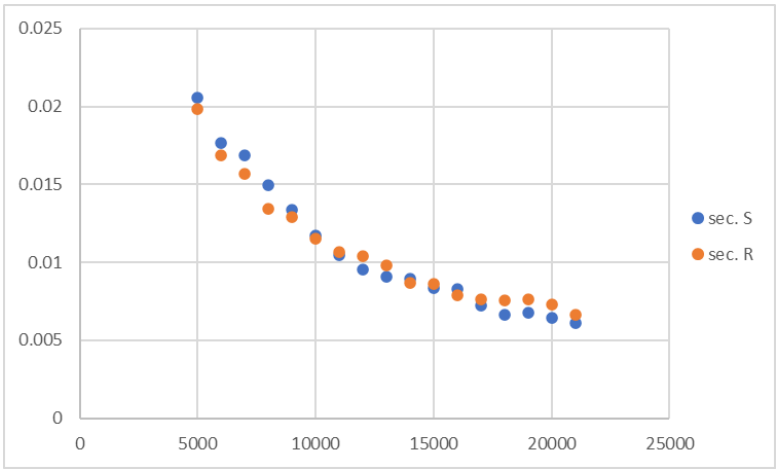

Secondary losses are higher for low rotational speeds, because low h/d ratio is lower. This means higher weight of the boundary layer at the tip and at the hub. Besides, the shorter the blade the higher will be the weight of the tip clearance leakage.

4.1.6 Annulus losses

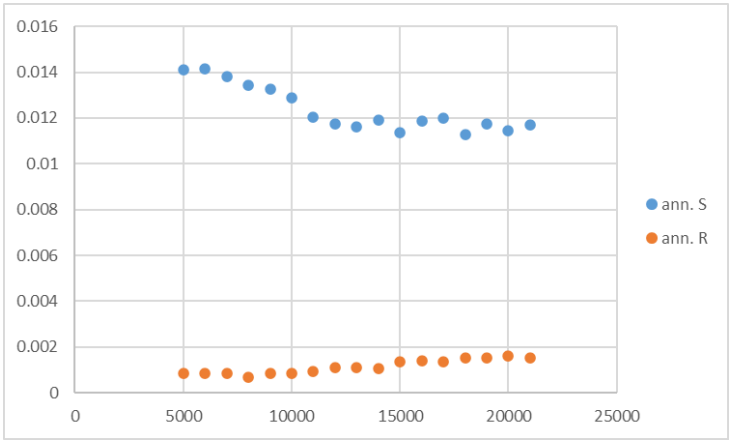

As seen before these losses are relevant for the stator and very little for the rotor. For the stator they decrease with the rotational speed. Being the axial velocities and the volume flow rate increase higher for higher speeds, the flow is less able to change direction in the unguided space between the rows. The opposite phenomenon occurs for the rotor.

4.1.7 Leakage losses

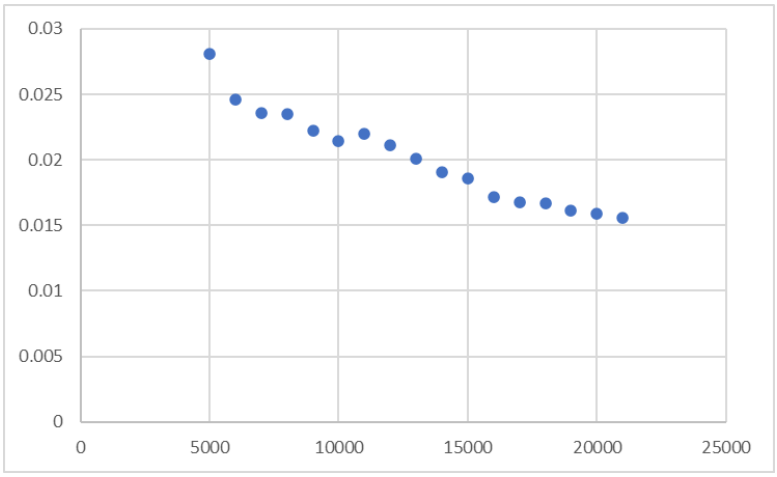

The decreasing trend is explainable with the fact that increasing the rotational speed h/D increases. For higher h/D values the leakage becomes less significant with respect to the rest of the flow.

4.1.8 Disk windage losses

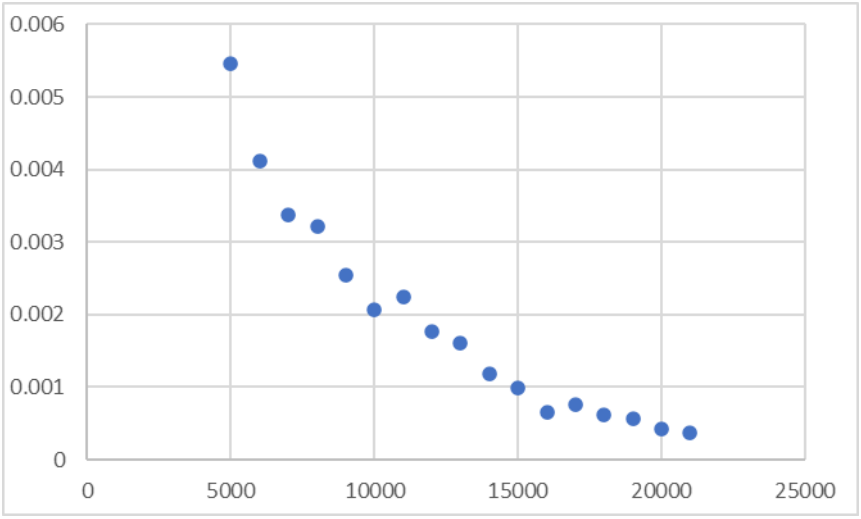

Disk windage is a viscous phenomenon that take place in the gap between the stationary and rotating disks. The fluid moves into the wheel cavities and is actioned by the rotor itself. This generates a boundary layer and the viscous forces break the rotating wheel, giving rise to loss.

4.1.9 Cumulative losses

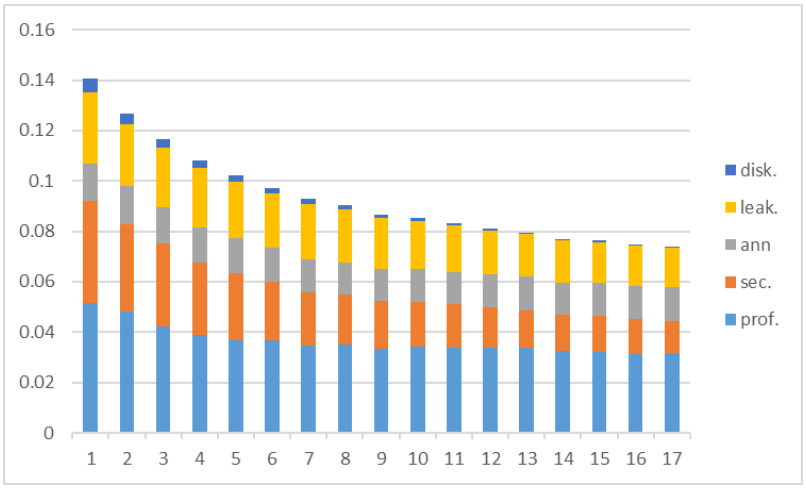

The following graph summarized all the losses described above. To be noted that kinetic energy losses are 0 for every rotational speed because the only first stage of the machine is considered that is followed by other stages that recuperate all the kinetic energy at the outlet of it.
The minimum of the cumulative losses is where the efficiency is at its maximum.